



Tectonic Influence on the Geomorphology of Submarine Canyons: Implications for Deep-Water Sedimentary Systems

Laura H. Bührig^{*†}, Luca Colombera[‡], Marco Patacci[‡], Nigel P. Mountney[‡] and William D. McCaffrey[‡]

School of Earth and Environment, Institute of Applied Geoscience, University of Leeds, Leeds, United Kingdom

OPEN ACCESS

Edited by:

Rosanna Maniscalco,
University of Catania, Italy

Reviewed by:

Daniele Casalbore,
Sapienza University of Rome, Italy
Andrea Fildani,
Deep Time Institute, United States

*Correspondence:

Laura H. Bührig
lhbuehrig@gmail.com

[†]This author has first authorship

[‡]These authors have contributed
equally to this work and share senior
authorship

Specialty section:

This article was submitted to
Quaternary Science, Geomorphology
and Paleoenvironment,
a section of the journal
Frontiers in Earth Science

Received: 15 December 2021

Accepted: 21 April 2022

Published: 02 June 2022

Citation:

Bührig LH, Colombera L, Patacci M,
Mountney NP and McCaffrey WD
(2022) Tectonic Influence on the
Geomorphology of Submarine
Canyons: Implications for Deep-Water
Sedimentary Systems.
Front. Earth Sci. 10:836823.
doi: 10.3389/feart.2022.836823

A database-informed metastudy of 294 globally distributed submarine canyons has been conducted with the aim of elucidating the role of tectonic setting on submarine-canyon geomorphology. To achieve this, data from seafloor and subsurface studies derived from 136 peer-reviewed publications and from open-source worldwide bathymetry datasets have been statistically analyzed. In particular, relationships between margin type (active vs. passive) or plate-boundary type (convergent vs. transform vs. complex) have been assessed for key morphometric parameters of submarine canyons, including: streamwise length, maximum and average width and depth, canyon sinuosity, average canyon thalweg gradient, and maximum canyon sidewall steepness. In addition, possible scaling relationships between canyon morphometric parameters and characteristics of the associated terrestrial catchment, continental shelf and slope, and of the broader physiographic setting for canyons along both active and passive margins have been evaluated. The following principal findings arise: 1) overall canyon geomorphology is not markedly different across tectonic settings; 2) slope failure might be more important in passive-margin canyons compared to active ones, possibly due to seismic strengthening in the latter; 3) some aspects of canyon geomorphology scale with attributes of the source-to-sink system and environmental setting, but the strength and sign in scaling might differ between active and passive margins, suggesting that the extent to which canyon geomorphology can be predicted depends on the tectonic setting. Insights from our analysis augment and improve conceptual, experimental and numerical models of slope systems at the scale of individual canyons and source-to-sink systems, and increase our understanding of the complex role played by tectonic setting in shaping deep-water systems.

Keywords: global, quantitative analysis, geometry, scaling relationships, source-to-sink, active margin, passive margin

1 INTRODUCTION

As major conduits for the exchange of sediment, organic matter, nutrients, pollutants and water masses across continental margins (e.g., Fildani, 2017; Santora et al., 2018; Maier et al., 2019; Zhong and Peng, 2021), submarine canyons are important components of deep-water environments and of broader source-to-sink (S2S) systems.

Canyon fills and deep-water fans collectively provide a depositional record of the sediment funneled through a connected canyon, and hold valuable information on the long-term evolution of continental margins (e.g., Normark and Carlson, 2003; Hessler and Fildani, 2019). They are more likely preserved when small in size, accommodated on continental crust, and associated with an active-margin setting (e.g., Normark et al., 1993; Normark and Carlson, 2003); this creates bias in the sedimentary record of deep-water systems. As a consequence, insights from ancient systems only provide a selective view on controls on deep-water systems and have limited applicability to modern environments. Moreover, current knowledge of the role of submarine-canyon geomorphology in shaping the configuration of deep-water systems largely relies on insights from a small number of modelling studies based on datasets from passive-margin settings (e.g., Wan et al., 2021) and a small number of comparative global studies with focus on specific aspects of canyon geomorphology (e.g., Normark and Carlson, 2003; Covault et al., 2011a). Furthermore, despite the importance of canyons for the delivery of sediment to deep-water basins, relationships between the geometry of submarine canyons and linked controls have not yet been fully considered in source-to-sink models; previous analyses were limited to the assessment of scaling relationships between canyon morphometric parameters with attributes of terrestrial catchments and continental shelves and slopes, which demonstrate that canyon geomorphology is partially controlled by the configuration of S2S systems (e.g., Sømme et al., 2009; Casalbore et al., 2011; Nyberg et al., 2018; Bührig et al., in review).

The quantitative investigation of modern canyons can increase our understanding of the importance of tectonic controls on their geomorphology, and in turn of the potential role of canyon geomorphology on sediment dispersal to deep-marine sinks. Insights in such relationships may also be useful for the reconstruction and prediction of geometries of deep-water systems and superordinate S2S systems, where these are only partially preserved in outcrop or are partially resolved in surveys of the seafloor and subsurface.

Submarine-canyon geomorphology is governed by multiple environmental factors including their hydrodynamic regime, oceanographic environment, regional climate, and tectonic setting (e.g., Harris and Whiteway, 2011; Huang et al., 2014; Puig et al., 2014; Bührig et al., in review), which control mechanisms of sediment routing from terrestrial source areas to marine sinks. In active-margin settings, relatively steep gradients and short transport distances across terrestrial catchments and the adjoining continental shelf promote rapid delivery of solids from the terrestrial hinterland to the deep-marine environment (e.g., Bouma and Scott, 2003; Sømme et al., 2009; Gamberi et al., 2015; Nyberg et al., 2018; Pierdomenico

et al., 2019). In systems with wide shelves along passive margins, sediment routing to slopes and basin floors is facilitated *via* shelf channels, shelf-edge deltas and submarine canyons that have cut across the shelf to connect to a river (e.g., Sylvester et al., 2012; Rona et al., 2015).

Some global studies indicate that the overall geomorphology of canyons might not differ fundamentally between tectonically active and passive margins (e.g., Harris and Whiteway, 2011; Bührig et al., in review). Yet tectonic activity molds the basin topography *via* its control on the distribution and type of faulting and mass-failures, which have been shown to leave characteristic signatures in the morphology of submarine canyons of active continental margins (e.g., Greene et al., 1991; Chiang and Yu, 2006; Micallef et al., 2014; Corradino et al., 2021; Soutter et al., 2021). Moreover, active margins encompass both convergent and strike-slip tectonic domains, and are characterized by variability in sedimentary basin-morphology and sediment generation, transport and dispersal mechanisms (e.g., Ingersoll, 2012; Ju et al., 2020). Although tectonically active margins host over 50% of submarine canyons globally (Harris and Whiteway, 2011), studies of the genesis and evolution of submarine canyons associated with active margins are relatively underrepresented in the scientific literature (Micallef et al., 2014).

The aim of this study is to increase understanding of the influence of tectonic setting on the geomorphology of submarine canyons. To achieve this, the geomorphology of 294 modern canyons has been investigated in their S2S context, considering parameters describing their physiographic and tectonic setting. Specific research objectives are as follows: 1) to quantitatively characterize the variability in selected canyon geomorphologic parameters across active (both convergent and strike-slip) and passive continental-margin types; 2) to evaluate scaling relationships in canyon morphometry and of individual canyon morphometric parameters with attributes describing their environmental setting, discriminating between active and passive margins; 3) to assess the characteristics of canyon-associated terrestrial catchments, shelves and slopes in active-versus passive-margin settings, and their scaling relationships.

2 DATASET AND METHODS

2.1 Dataset

The dataset used in this study has been extracted from a database of submarine canyons collated by Bührig et al. (in review), who have investigated controlling factors on canyon geomorphology in a global metastudy. For the present study, the database has been extended by defining and characterizing new attributes and by integration with additional data to facilitate the analyses. The data presented in this article are made available in the Supplementary Material.

Data on the geomorphology of the canyons have been extracted from high-resolution seabed and subsurface studies from 136 peer-reviewed publications and from open-source worldwide bathymetry (NOAA National Centers for Environmental Information, 2021; Google Earth). The dataset is organized as 97 individual case studies, with each case

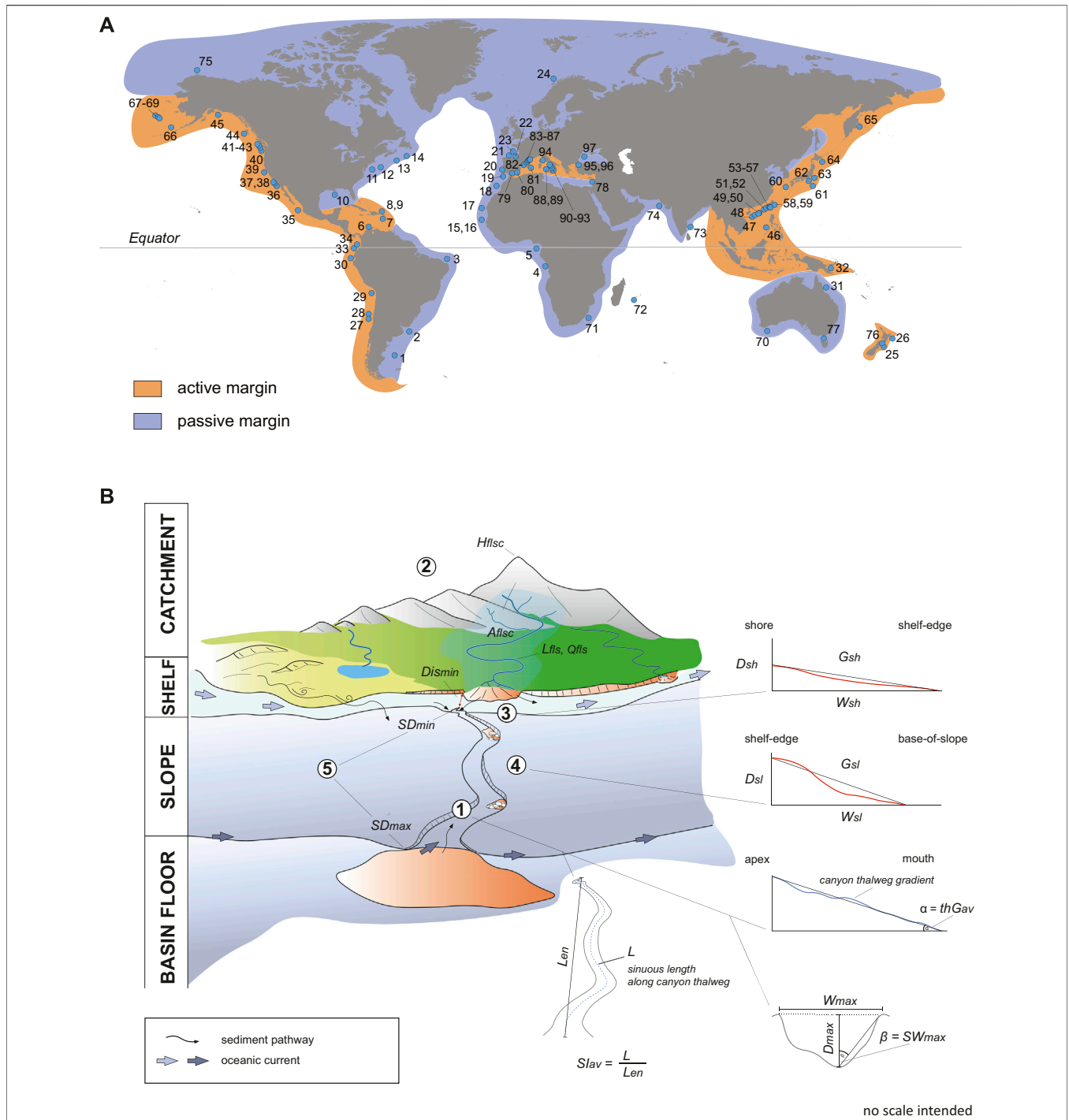


FIGURE 1 | (A) Overview map of the distribution of the 97 case studies and their associated margin-type setting. Continental-margin classification after Harris et al. (2014b) (World map from freevectormaps.com). **(B)** Key parameters investigated in the study: 1) Submarine canyon: L , canyon length along thalweg; L_{en} , canyon length along endpoints; W_{max} , maximum canyon width; D_{max} , maximum canyon depth; S_{lav} , average canyon sinuosity index; thG_{av} , average canyon thalweg gradient; SW_{max} , maximum canyon sidewall steepness. 2) Terrestrial catchment: L_{fls} , fluvial system length; Q_{fls} , average annual fluvial discharge; A_{flsc} , catchment size; H_{flsc} , maximum catchment elevation. 3) Shelf configuration: W_{sh} , shelf width; D_{sh} , shelf-break depth; G_{sh} , average shelf gradient. 4) Slope configuration: W_{sl} , slope width; D_{sl} , slope-break depth; G_{sl} , average slope gradient. 5) Canyon-physiographic setting: SD_{min} , seafloor depth at canyon apex; SD_{max} , seafloor depth at canyon mouth; Dis_{min} , minimum distance of canyon to shoreline.

TABLE 1 | Summary of the 97 case studies considered in this study.

ID	Case study	No. of canyons	Oceanic region	Reference(s)
1	Patagonia canyons, SE Argentina	8	South Atlantic Ocean	Lastras et al. (2011a)
2	Mar del Plata Canyon, E Argentina	1	South Atlantic Ocean	Krastel et al. (2011), Warratz et al. (2019)
3	Potiguar Basin canyons, NE Brazil	14	South Atlantic Ocean	de Almeida et al. (2015)
4	Congo Canyon, W Democratic Republic of Congo	1	South Atlantic Ocean	Babonneau et al. (2002), Ferry et al. (2004)
5	Avon & Mahin canyons, SW Nigeria	2	South Atlantic Ocean	Jimoh et al. (2018)
6	Aguja Canyon, N Colombia	1	North Atlantic Ocean (Caribbean Sea)	Restrepo-Correa and Ojeda (2010)
7	Guayanilla canyon system, S Puerto Rico	4	North Atlantic Ocean (Caribbean Sea)	Trumbull and Garrison (1973)
8	Arecibo & Quebradillas canyons, NW Puerto Rico	2	North Atlantic Ocean	Gardner et al. (1980)
9	Mona Canyon, NW Puerto Rico	1	North Atlantic Ocean	Mondziel et al. (2010)
10	Mississippi Canyon, S United States	1	North Atlantic Ocean (Gulf of Mexico)	Coleman et al. (1982)
11	Hudson Canyon, NE United States	1	North Atlantic Ocean	Rona et al. (2015)
12	Lydonia & Oceanographer canyons, NE United States	2	North Atlantic Ocean	Valentine et al. (1980)
13	Logan Canyon, SE Canada	1	North Atlantic Ocean	Li et al. (2019)
14	SW Grand Banks Slope canyons, SE Canada	3	North Atlantic Ocean	Armitage et al. (2010)
15	Dakar Canyon, W Senegal	1	North Atlantic Ocean	Pierau et al. (2010), Pierau et al. (2011)
16	Cayar Canyon, W Senegal	1	North Atlantic Ocean	Dietz et al. (1968)
17	Timiris Canyon, NW Mauritania	1	North Atlantic Ocean	Krastel et al. (2004), Antobreh and Krastel (2006)
18	Agadir Canyon	1	North Atlantic Ocean	Ercilla et al. (1998), Wynn et al. (2002)
19	Faro & Portimao canyons, SW Portugal	2	North Atlantic Ocean (Gulf of Cadiz)	Mulder et al. (2006)
20	Nazaré, Cascais & Setubal-Lisbon canyons, W Portugal	4	North Atlantic Ocean	Arzola et al. (2008), Lastras et al. (2009), Allin et al. (2016)
21	Aviles Canyon system & Navia canyon, N Spain	5	North Atlantic Ocean (Bay of Biscay)	Gómez-Ballesteros et al. (2014)
22	Capbreton Canyon, SW France	1	North Atlantic Ocean (Bay of Biscay)	Mazières et al. (2014)
23	Audierne & Blackmud canyons, SW France	2	North Atlantic Ocean (Bay of Biscay)	Mulder et al. (2012)
24	Lofoten-Vesterålen canyons (incl. Andøya Canyon), NW Norway	15	North Atlantic Ocean	Rise et al. (2013)
25	Kaikoura Canyon, E New Zealand	1	South Pacific Ocean	Lewis and Barnes (1999)
26	Lachlan Canyon, NE New Zealand	1	South Pacific Ocean	Walsh et al. (2007)
27	Biobío Canyon system, SW Chile	2	South Pacific Ocean	Bernhardt et al. (2015)
28	San Antonio Canyon, NW Chile	1	South Pacific Ocean	Hagen et al. (1996), Laursen and Normark (2002)
29	E Arequipa Basin canyons, NW Chile	3	South Pacific Ocean	Hagen et al. (1994)
30	Guayaquil & Santa Elena canyons, NW Ecuador	2	South Pacific Ocean	Michaud et al. (2015)
31	N Great Barrier Reef canyons, NE Australia	15	South Pacific Ocean (Coral Sea)	Puga-Bernabéu et al. (2011)
32	Solomon Sea canyons, E & SE Papua New Guinea	8	South Pacific Ocean (Solomon Sea)	Davies et al. (1987), Galewsky and Silver (1997)
33	Esmeraldas Canyon, NW Ecuador	1	North Pacific Ocean	Michaud et al. (2015)
34	Mira & Patia canyons, SW Colombia	2	North Pacific Ocean	Ratzov et al. (2012)
35	Ipala Canyon, W Mexico	1	North Pacific Ocean (South China Sea)	Urías Espinosa et al. (2016)
36	La Jolla, Scripps, Sur, Carmel, Noyo & Eel canyons, SW United States	6	North Pacific Ocean	Le Dantec et al. (2010), Paull et al. (2013)
37	Redondo, Santa Monica & Dume canyons, SW United States	3	North Pacific Ocean	Gardner et al. (2003), Tubau et al. (2015)
38	Mugu & Hueneme canyons, SW United States	2	North Pacific Ocean	Piper et al. (1999)
39	Monterey, Soquel, Año Nuevo & Cabrillo canyons, SW United States	4	North Pacific Ocean	Greene et al. (2002), Xu and Noble (2009)
40	Astoria Canyon, NW United States	1	North Pacific Ocean	Hickey (1997), Bosley et al. (2004)
41	Quinault Canyon, NW United States	1	North Pacific Ocean	Baker and Hickey (1986), Carson et al. (1986)
42	Juan de Fuca Canyon, NW United States	1	North Pacific Ocean (heads in the Juan de Fuca Strait)	Alford and MacCready (2014)
43	Barkley Canyon, SW Canada	1	North Pacific Ocean	Allen et al. (2001)
44	Haida Gwaii canyons, SW Canada	6	North Pacific Ocean	Harris et al. (2014a)
45	Tarr Canyon, NW United States	1	North Pacific Ocean (Gulf of Alaska)	Carlson et al. (1990)
46	North Palawan Canyon, S China	1	North Pacific Ocean (South China Sea)	Yin et al. (2018)
47	Modern Central Canyon, S China	1	North Pacific Ocean (South China Sea)	Su et al. (2015)
48	3 canyons & 4 gullies, S China	3 (4)	North Pacific Ocean (South China Sea)	Chen et al. (2017)
49	Pearl River Mouth Basin canyons, S China	17	North Pacific Ocean (South China Sea)	Han et al. (2010), Su et al. (2020)
50	Zhujiang/Pearl River Canyon, S China	1	North Pacific Ocean (South China Sea)	Han et al. (2010), Ding et al. (2013)
51	Dongsha Canyon, S China	1	North Pacific Ocean (South China Sea)	Yin et al. (2015)
52	Taiwan Canyon, SW Taiwan	1	North Pacific Ocean (South China Sea)	Xu et al. (2014)
53	Hongtsai Canyon, SW Taiwan	1	North Pacific Ocean (South China Sea)	Yu and Chiang (1995)
54	Fangliao Canyon, SW Taiwan	1	North Pacific Ocean (South China Sea)	Yu and Lu (1995), Chiang et al. (2012)
55	Kaoping Canyon, SW Taiwan	1	North Pacific Ocean (South China Sea)	Chiang and Yu (2006), Liu et al. (2016)
56	Kaohsiung Canyon, SW Taiwan	1	North Pacific Ocean (South China Sea)	Yu et al. (1992)

(Continued on following page)

TABLE 1 | (Continued) Summary of the 97 case studies considered in this study.

ID	Case study	No. of canyons	Oceanic region	Reference(s)
57	Penghu Canyon, SW Taiwan	1	North Pacific Ocean (South China Sea)	Yu and Chang (2002), Hsiung and Yu (2011), Su et al. (2015)
58	Taitung Canyon, SE Taiwan	1	North Pacific Ocean (Philippine Sea)	Schnürle et al. (1998)
59	Hualien Canyon, SE Taiwan	1	North Pacific Ocean (Philippine Sea)	Hsiung et al. (2017)
60	Goto Canyon, SW Japan	1	North Pacific Ocean (East China Sea)	Oiwane et al. (2011)
61	Aoga Shima Canyon, SE Japan	1	North Pacific Ocean (Philippine Sea)	Klaus and Taylor (1991)
62	Tenryu Canyon, SE Japan	1	North Pacific Ocean	Soh and Tokuyama (2002)
63	Boso Canyon, SE Japan	1	North Pacific Ocean	Soh et al. (1990)
64	Kushiro Canyon, NE Japan	1	North Pacific Ocean	Noda et al. (2008), Noda and Tuzino (2010), Tuzino and Noda (2010)
65	Submarine canyons of Kamchatka, NE Russia	7	North Pacific Ocean	Gribidenko and Svarichevskaya (1984)
66	Bering Canyon, Bering Sea	1	North Pacific Ocean (Bering Sea)	Carlson and Karl (1988), Harris and Whiteway (2011)
67	Zhemchug, Pervenets & Navarin canyons, Bering Sea	3	North Pacific Ocean (Bering Sea)	Carlson and Karl (1988)
68	Middle canyon system, Bering Sea	2	North Pacific Ocean (Bering Sea)	Carlson and Karl (1984), Carlson and Karl (1988)
69	St. Matthew canyon system, Bering Sea	2	North Pacific Ocean (Bering Sea)	Carlson and Karl (1984), Carlson and Karl (1988)
70	Albany canyons, SW Australia	11	Indian Ocean	Exon et al. (2005)
71	Tugela Canyon, E South Africa	1	Indian Ocean	Wiles et al. (2013)
72	Saint-Etienne & Pierrefonds canyons, SW La Reunion	2	Indian Ocean	Babonneau et al. (2013)
73	Palar Basin canyons, E India	20	Indian Ocean	Susanth et al. (2021)
74	Indus Canyon, SE Pakistan	1	Indian Ocean (Arabian Sea)	Von Rad and Tahir (1997), Salmanidou et al. (2019)
75	Barrow Canyon, NW United States	1	Arctic Ocean	Eittreim et al. (1982), Pisareva et al. (2019)
76	Cook Strait canyons, E New Zealand	9	Cook Strait	Mountjoy et al. (2009), Mountjoy et al. (2014), Micallef et al. (2014)
77	Bass canyon system, SE Australia	10	Bass Strait	Mitchell et al. (2007)
78	Akhviz & Sour canyons, NW Israel	2	Mediterranean Sea	Mart (1989), Almagor (1993)
79	Almeria, Western, Eastern & Guadiaro canyons, S Spain	4	Mediterranean Sea	Alonso and Ercilla (2003), Palanques et al. (2005)
80	Alías-Almanzora canyon system, SE Spain	4	Mediterranean Sea	Puig et al. (2017)
81	Menorca Canyon, SW Menorca, Balearic Islands	1	Mediterranean Sea	Acosta et al. (2002)
82	Orpesa Canyon, NE Spain	1	Mediterranean Sea	Amblas et al. (2012)
83	Foix Canyon system, NE Spain	3	Mediterranean Sea	Puig et al. (2000), Tubau et al. (2013)
84	Blanes Canyon, SE France	1	Mediterranean Sea	Lastras et al. (2011b)
85	Palamós/La Fonera Canyon, NE Spain	1	Mediterranean Sea	Martin et al. (2006), Palanques et al. (2006), Lastras et al. (2011b)
86	Cap de Creus Canyon, NE Spain	1	Mediterranean Sea	Baztan et al. (2005), Lastras et al. (2007), Lastras et al. (2011b)
87	Bourcart Canyon, SE France	1	Mediterranean Sea	Mauffrey et al. (2015)
88	Gulf of Palermo canyons, NW Sicily, Italy	7	Mediterranean Sea	Lo Iacono et al. (2011), Lo Iacono et al. (2014)
89	Gulf of Castellammare canyons, NW Sicily, Italy	2	Mediterranean Sea	Lo Iacono et al. (2014)
90	Messina Canyon, NE Sicily, Italy	1	Mediterranean Sea	Ridente et al. (2014)
91	Petrace, Gioia & Mesima canyons, SW Italy	3	Mediterranean Sea	Pierdomenico et al. (2016), Casalbone et al. (2018)
92	Luna & Infreschi canyons, SW Italy	2	Mediterranean Sea	Budillon et al. (2011)
93	Dohrn Canyon, SW Italy	1	Mediterranean Sea	Milia (2000)
94	Golo system canyons, NE Corsica, France	4 (2)	Mediterranean Sea	Gervais et al. (2004), Gervais et al. (2006)
95	North İmralı Canyon, NW Turkey	1	Sea of Marmara	Vardar (2019)
96	Sarköy & Izmit canyons, NW Turkey	2	Sea of Marmara	Çağatay et al. (2015)
97	Danube/Viteaz Canyon, SE Romania	1	Black Sea	Popescu et al. (2004)

The numbers of canyons reported in brackets indicate channel forms that were termed as "submarine gullies" by the authors of the original data sources.

corresponding to one or several submarine canyons from a geographic location or region, detailed as a self-contained study by the original authors (**Figure 1A**; **Table 1**).

2.2 Methods

Data on individual canyon morphometric parameters, the physiographic setting of the canyon and characteristics of its associated S2S system have been coded in the Deep-Marine

Architecture Knowledge Store (DMAKS; Cullis et al., 2019), a relational database storing data on characteristics of deep-water sedimentary systems and their environmental settings (see Cullis et al., 2019).

2.2.1 Canyon Definition

In this study, a submarine canyon is defined as a throughgoing erosional channel form incised into the continental slope; this

TABLE 2 | Overview of the parameters investigated in the study and their definitions.

Study parameter	Definition
Canyon morphometrics	
L (km)**	Streamwise length of the canyon between canyon apex and canyon mouth as measured along the canyon thalweg
W_{max} (km)**	Maximum width of the canyon orthogonal to the canyon length
W_{av} (km)*	Average canyon width over the length of the entire canyon
D_{max} (m)*	Maximum depth of the canyon, i.e., depth of the canyon thalweg relative to the elevation of the canyon margins
D_{av} (m)*	Average canyon thalweg depth over the length of the entire canyon
S_{lav} (-)**	Average canyon sinuosity index, i.e., ratio between the sinuous canyon length measured along its thalweg and the straight distance between canyon apex and canyon mouth
thG_{av} (°)**	Average canyon thalweg gradient, evaluated between canyon apex and canyon mouth
SVW_{max} (°)*	Maximum canyon-sidewall steepness, representing the maximum value of gradient between canyon rim and canyon bottom evaluated along the entire length of the canyon
Physiographic setting	
Dis_{min} (km)**	Minimum distance between the canyon and the shoreline
SD_{min} (m)**	Seafloor depth at the top of the canyon
SD_{max} (m)**	Seafloor depth at the mouth of the canyon
Canyon terrestrial catchment	
L_{fis} (km)**	Length of the river with a present-day or previous connection with the canyon, from headwater to river mouth; for canyons connected with several rivers the cumulative length has been considered
Q_{fis} (km ³ /yr)*	Mean annual discharge of the fluvial system; for canyons connected with several rivers the cumulative mean annual discharge has been considered
A_{fisc} (km ²)*	Size of the catchment associated with the fluvial system; for canyons connected with several rivers the cumulative catchment area size has been considered
H_{fisc} (m)**	Maximum elevation of the catchment associated with the fluvial system; for canyons connected with several rivers, the elevation of the highest peak in the combined catchments has been considered
Continental shelf	
W_{sh} (km)**	Width of the shelf at the canyon location
G_{sh} (°)**	Average shelf gradient at the canyon location
D_{sh} (m)**	Shelf-break depth at the canyon where the shelf edge is intact and not eroded into by the latter; for shelf edges displaying some degree of variability in their bathymetry the maximum depth of the shelf break has been chosen
Continental slope	
W_{sl} (km)**	Width of the slope at the canyon location
G_{sl} (°)**	Average slope gradient between the shelf break and the slope break
D_{sl} (m)**	Slope-break depth at the canyon
Other parameters	
Continental-margin type	For canyons located along continental margins, including canyons associated with islands: 1) active margin, including transform margins; 2) passive margin [classification after Figure 2 of Harris et al. (2014b)]
Active-margin plate boundary type	Based on the type of plate boundary, active margins are distinguished into 1) convergent, 2) transform, and 3) complex margins. The latter category includes settings which involve more than one plate boundary, and margins which display an additional direction of motion, e.g., convergent margins with a transform component

definition does not therefore consider ancillary criteria that are sometimes used by some authors, such as their origin or minimum size (cf. Harris and Whiteway, 2011). The general definition used herein encompasses smaller channelforms, which are sometimes referred to as “submarine gullies” (e.g., Gervais et al., 2006), “submarine gulley” (e.g., Normark et al., 2009) or “potential submarine canyons” (e.g., de Almeida et al., 2015), and which might represent forms at the early stage of development of a canyon (e.g., Nelson et al., 2011; Sanchez et al., 2012; Amblas et al., 2017 and references therein). The terms “canyon” and “gully” (or “gulley”) are not clearly distinguished in terms of size in the wider literature, and both terms are used when referring to smaller channelforms.

2.2.2 Study Parameters

2.2.2.1 Canyon Morphometrics

Canyon geomorphology has been assessed based on the following morphometric parameters: streamwise canyon length, maximum and average canyon width and depth, canyon sinuosity, average

canyon thalweg gradient, and maximum canyon sidewall steepness. Values reported in textual form in the literature sources have only been considered where underpinned by observations on bathymetric surveys with full coverage of the canyon.

2.2.2.2 Physiographic Setting

The physiographic setting of the studied canyons has been characterized by means of attributes describing the bathymetry of the canyon apex and mouth, and the minimum distance of the canyon to the shoreline.

2.2.2.3 Source-to-Sink System Attributes

For canyons with a present or past sediment connection with a fluvial system, the length and average annual water discharge of the river have been recorded, as well as the size and maximum elevation of its catchment. In cases where canyons are linked with several rivers, the sum of the length of the individual rivers, the sum of their mean annual fluvial discharges and catchment areas, and the maximum

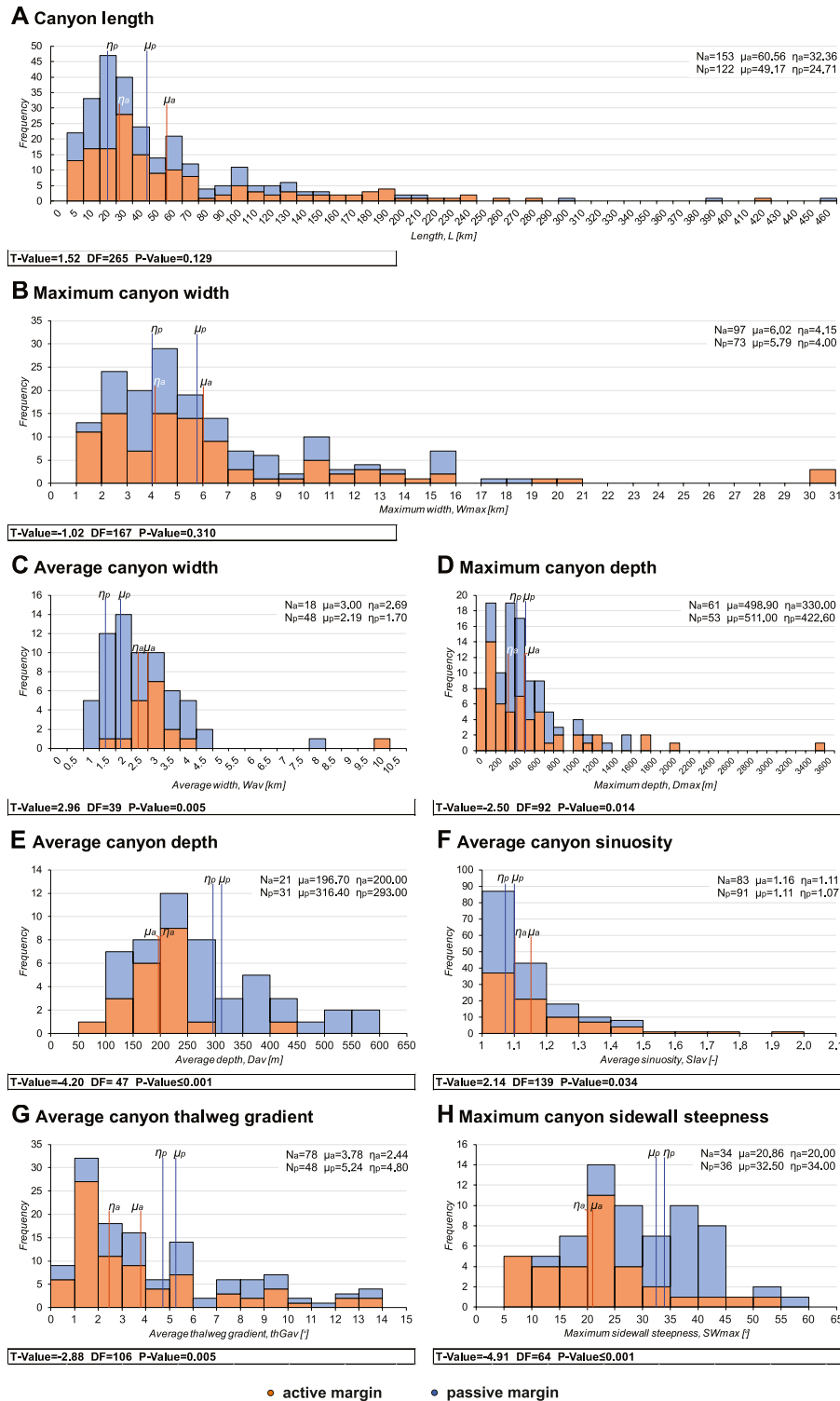


FIGURE 2 | (A–H) Stacked histograms of morphometric values in studied canyons in active (a) vs. passive (p) margins. N , number of readings; μ = mean value; η = median value; DF, degrees of freedom.

elevation of the highest peak in the combined catchments have been recorded; this enables comparison with canyons fed by single fluvial systems. The geometric configuration of the continental margin at the

canyon location has been characterized in terms of average gradient of shelf and slope, and depth of shelf break and base of slope below present-day mean sea level.

2.2.2.4 Tectonic Setting

Canyon-hosting continental margins have been classified as active or passive following the classification by Harris et al. (2014b) (see **Figure 1A**). Active margins have been further differentiated based on the plate-boundary type with which they are associated, as convergent, transform and complex margins. The term “complex” is used here to refer to settings that involve more than one type of plate boundary and sense of motion (e.g., convergent margins with a transform component).

Definitions of the studied parameters are provided in **Table 2** and illustrated in **Figure 1B**.

2.3 Statistical Analyses

Different types of statistical analyses have been conducted to evaluate scaling relationships within submarine canyons, and between canyon geomorphology and attributes of its environment as a function of the tectonic setting.

- 1) *Descriptive statistics*: Frequency distributions of the studied canyon morphometric parameters have been summarized in terms of minimum, maximum, mean and median values, to reveal differences across margin types and active-margin plate boundary types.
- 2) *Hypothesis testing*: Hypothesis testing has been used to evaluate the statistical significance of differences in mean values of canyon morphometric parameters across classes of canyons for different tectonic settings and attributes of the source-to-sink system along active and passive margins. The Welch’s two sample t-test (only referred to as “t-test” hereafter) has been used for comparisons between active and passive margins; Welch’s ANOVA (only “ANOVA” hereafter) has been used for comparisons between convergent, transform and complex plate-boundary settings of active margins. The chosen tests allow testing of datasets with non-equal variances. For skewed frequency distributions, a logarithmic variable transformation has been conducted prior to the analyses. In these instances, where differences in mean values are reported in the text, they refer to the transformed variables and not the variables themselves. To enable a pairwise comparison of mean values between the three different active-margin settings, ANOVA has been complemented with Games-Howell post-hoc tests. Test statistics (t-test: *T*-value; ANOVA: *F*-value; Games-Howell: *T*-value), *p*-values and degrees of freedom (DF) are presented for all tests below each individual figure. To limit the number of false positives, the confidence interval has been set at 99%, with results where *p*-values are ≤ 0.01 treated as statistically significant.
- 3) *Correlation analysis*: Correlation analyses have been undertaken to assess pairwise scaling relationships between study parameters. Correlation coefficients quantify the sign and strength of correlation: the Pearson’s correlation coefficient (*r*) describes linear relationships, whereas Spearman’s rank correlation coefficient (r_s) describes monotonic relationships. The statistical significance of a correlation between two variables is indicated by *p*-values. A confidence interval of 99% is employed to indicate significant correlations.

2.4 Limitations of the Study

Data analyses and interpretations are subject to some limitations, including the following:

- 1) Metastudies might inherit unidentified data errors from the original literature data sources. This has been minimized by exclusively considering data from peer-reviewed publications and government agency sources.
- 2) Although care has been taken to avoid potential bias in the geographic distribution of case studies (see Matos et al., 2018), some geographic bias may exist for canyons from transform margins specifically, which are only considered for two regions (offshore California, Sea of Marmara), both located at temperate latitudes.
- 3) Some statistical analyses are based on datasets of limited size. This is the case for data on morphometric parameters of canyons from transform and complex settings, but also for pairs of variables whose correlation is evaluated. Correlation analyses are typically only considered and discussed where the number of observations (*N*) is equal to or larger than 15, making it explicit when $N < 15$.
- 4) Some relationships might represent covariance related to factors that were not assessed in this study, but which may influence canyon geomorphology, such as lithology (e.g., Smith et al., 2017) and rate and direction of relative sea-level changes (e.g., Covault et al., 2011b), among others.

3 RESULTS

3.1 Scaling Between Canyon Morphometric Parameters and the Tectonic Setting

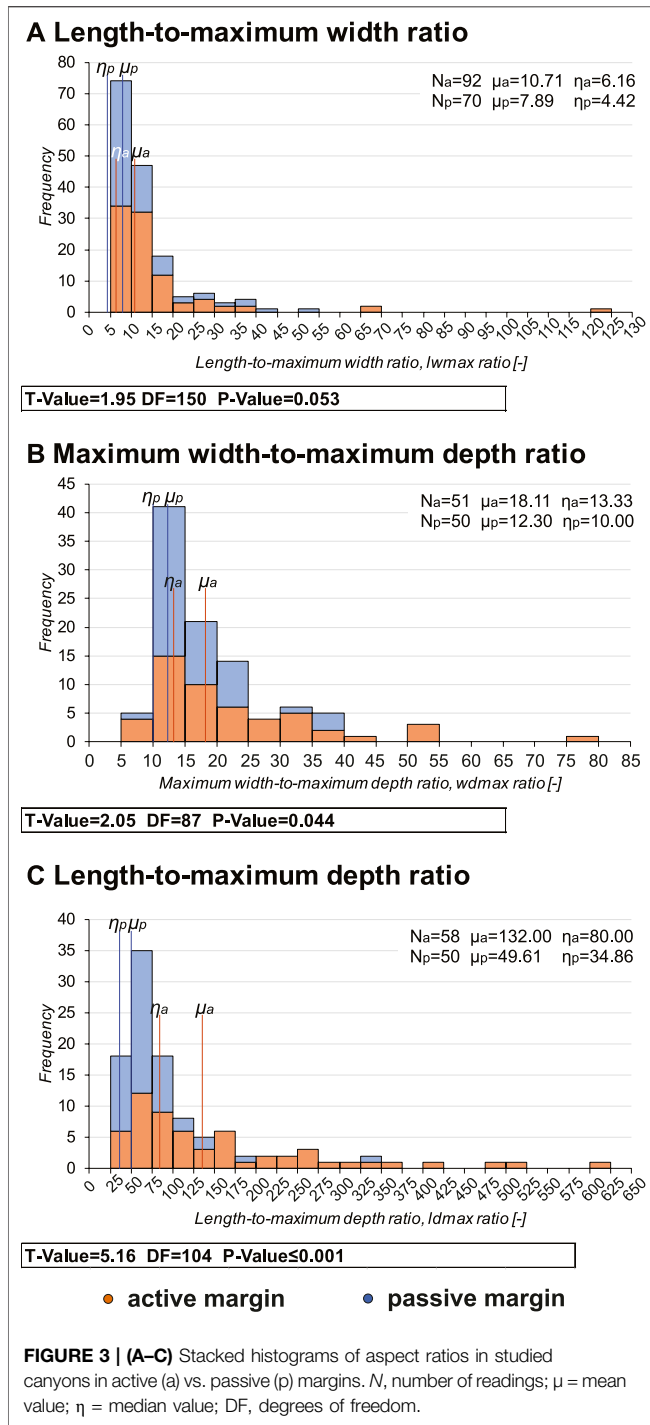
3.1.1 Continental-Margin Type

3.1.1.1 Canyon Dimensions and Aspect Ratios

Comparisons of the maximum and average dimensions of submarine canyons along tectonically active and passive margins demonstrate how canyon geometry varies between the two canyon groups.

Canyons in active margins are, on average, longer than those along passive margins—by a factor 1.23—but the difference in mean is not statistically significant. The longest canyon in the study is associated with a passive margin, but lengths of more than 400 km occur in both groups (**Figure 2A**). The deepest and widest canyons are seen on active margins. However, these values of depth and width represent individual outliers; ranges in maximum widths and depths are similar for the vast majority of studied canyons in both margin types, and their mean values are very similar (**Figures 2B,D**).

Canyons in the two margin types exhibit average widths within the same range. On average, mean canyon width is 1.37 times greater in studied active-margin examples, which show a narrower range in values than their counterparts from passive margins (**Figure 2C**). However, average-width data relating to canyons from an active-margin setting are associated with two case studies only, both from the South China Sea, whereas average width data for canyons in passive-margin settings are derived from examples from only three



geographic regions; therefore, these findings need to be corroborated by additional data in future research. In contrast, the mean average canyon depth is significantly greater for passive margins, by a factor 1.6. The maximum average depth of passive-margin canyons (594 m) is notably higher than that of active-margin ones (400 m) (Figure 2E).

Despite a greater range in aspect ratios of maximum canyon dimensions for examples from active margins, the mean values of

streamwise length-to-maximum width (lw_{max}) (Figure 3A) and maximum width-to-maximum depth (wd_{max}) (Figure 3B) ratios are similar for the two margin types. In contrast, a statistically significant difference in the mean value of length-to-maximum depth (ld_{max}) ratio (Figure 3C) is seen; this parameter is on average 2.66 times larger for active-margin canyons.

3.1.1.2 Average Canyon Sinuosity, Average Canyon Thalweg Gradient and Maximum Canyon Sidewall Steepness

The studied active-margin canyons show a greater range in average canyon sinuosity than passive-margin ones, but mean average canyon sinuosity is equally low in both margin types, ~1.1 (Figure 2F).

The range in average canyon thalweg gradient is very similar for the two margin types; thalwegs are, on average, steeper in the studied passive-margin examples to a statistically significant level (Figure 2G).

Canyons situated in passive settings have steeper canyon sidewalls compared to those in tectonically active settings. On average, the maximum sidewall gradient varies significantly between the two canyon groups, and is larger by a factor 1.56 for passive-margin examples (Figure 2H).

3.1.2 Active Margin Plate-Boundary Type

3.1.2.1 Canyon Dimensions and Aspect Ratios

Canyons in convergent settings display the highest maximum values of length, maximum width and depth. Yet, on average, maximum canyon dimensions are greater in canyons located at complex plate boundaries (Figures 4A–C). The maximum width (Figure 4B) and depth (Figure 4C) of canyons from this type of setting are on average significantly higher than that of canyons in convergent settings, by a factor of 1.77 and 1.29, respectively.

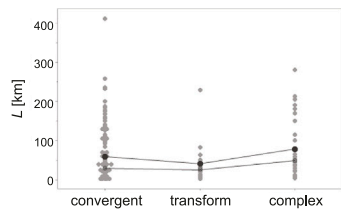
The length (Figure 4A) and maximum width (Figure 4B) of canyons along transform plate boundaries are, on average, lower than those of canyons in the other two settings. The mean canyon length does not vary significantly across the three active-margin settings (Figure 4A). Instead, the mean maximum canyon width differs at a statistically significant level between transform and complex settings (Figure 4B), but this variable could only be constrained for twelve transform-setting canyons. Although data on maximum canyon depth for canyons along transform plate boundaries could only be derived for four examples, the data demonstrate that the depth range of canyons in such settings is similar to that of canyons in convergent settings, and larger than that of canyons from complex settings (Figure 4C).

Mean aspect ratios are similar across all three active-margin settings, but relatively few data are available for canyons in transform- and complex-margin settings. Aspect ratios based on maximum canyon dimensions for canyons in convergent settings are highly variable and display the greatest range in values (Figures 4G–I).

3.1.2.2 Average Canyon Sinuosity, the Average Canyon Thalweg Gradient and Maximum Canyon Sidewall Steepness

Frequency distributions of average canyon sinuosity for convergent, transform and complex plate boundaries exhibit similar mean and median values. Based on results of Welch's

A Canyon length

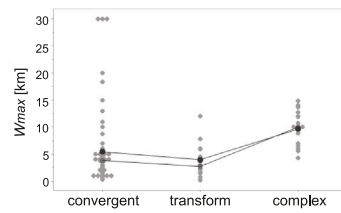


	N	min	mean	StDev	median	max
conv.	108	2,00	59,00	68,47	29,09	411,00
trans.	17	2,50	40,90	52,80	25,10	229,70
comp.	28	3,90	78,50	78,20	48,90	279,70

Welch's ANOVA
F-Value= 1.01 DF Num=2 DF Den=36.7576 P-Value=0.373

	Dmean	SE	T-Value	adjusted P-Value
conv. vs trans.	-0,100	0,119	-0,84	0,682
conv. vs comp.	0,118	0,119	1,00	0,584
comp. vs trans.	0,218	0,152	1,43	0,335

B Maximum canyon width

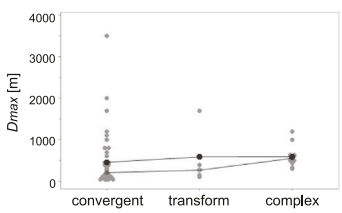


	N	min	mean	StDev	median	max
conv.	67	0,25	5,42	6,60	3,83	30,00
trans.	18	0,15	3,98	3,46	2,73	12,00
comp.	12	4,30	9,62	3,21	10,00	14,80

Welch's ANOVA
F-Value=25.72 DF Num=2 DF Den=27.0868 P-Value<0.001

	Dmean	SE	T-Value	adjusted P-Value
conv. vs trans.	-0,124	0,158	-0,78	0,718
conv. vs comp.	0,4356	0,0647	6,73	<0.001
comp. vs trans.	0,560	0,154	3,64	0,008

C Maximum canyon depth

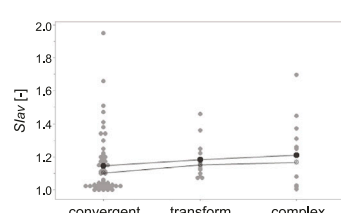


	N	min	mean	StDev	median	max
conv.	43	35,00	459,60	647,90	210,00	3500,00
trans.	4	110,00	588,00	752,00	270,00	1700,00
comp.	15	310,00	594,30	240,50	555,00	1200,00

Welch's ANOVA
F-Value=8.50 DF Num=2 DF Den=7.84612 P-Value=0.011

	Dmean	SE	T-Value	adjusted P-Value
conv. vs trans.	0,133	0,278	0,48	0,886
conv. vs comp.	0,3686	0,0865	4,26	<0.001
comp. vs trans.	0,236	0,271	0,87	0,690

D Average canyon sinuosity

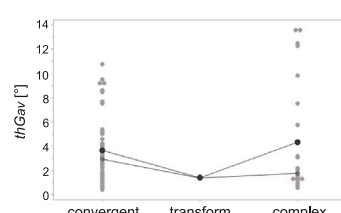


	N	min	mean	StDev	median	max
conv.	58	1,00	1,14	0,18	1,10	1,95
trans.	13	1,07	1,18	0,12	1,15	1,46
comp.	12	1,00	1,21	0,22	1,17	1,70

Welch's ANOVA
F-Value=0.94 DF Num=2 DF Den=22.2231 P-Value=0.405

	Dmean	SE	T-Value	adjusted P-Value
conv. vs trans.	0,0163	0,0139	1,18	0,477
conv. vs comp.	0,0222	0,0231	0,96	0,613
comp. vs trans.	0,0059	0,0245	0,24	0,969

E Average canyon thalweg gradient

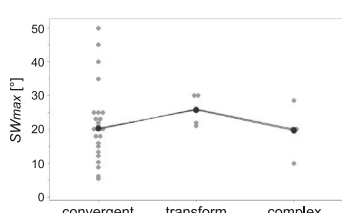


	N	min	mean	StDev	median	max
conv.	52	0,40	3,67	2,63	2,93	10,77
trans.	3	1,30	1,39	0,10	1,38	1,50
comp.	23	0,60	4,34	4,65	1,77	13,60

Welch's ANOVA
F-Value=21.66 DF Num=2 DF Den=37.9576 P-Value<0.001

	Dmean	SE	T-Value	adjusted P-Value
conv. vs trans.	-0,3078	0,0498	-6,18	<0.001
conv. vs comp.	-0,039	0,103	-0,38	0,924
comp. vs trans.	0,2686	0,0943	2,85	0,024

F Maximum canyon sidewall steepness

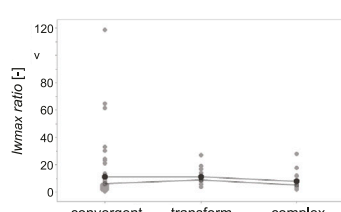


	N	min	mean	StDev	median	max
conv.	26	5,40	20,30	11,75	20,00	50,00
trans.	4	21,00	25,75	4,92	26,00	30,00
comp.	4	10,00	19,63	7,56	20,00	28,50

Welch's ANOVA
F-Value=1.47 DF Num=2 DF Den=7.23013 P-Value=0.291

	Dmean	SE	T-Value	adjusted P-Value
conv. vs trans.	5,45	3,37	1,62	0,285
conv. vs comp.	-0,68	4,43	-0,15	0,987
comp. vs trans.	-6,12	4,51	-1,36	0,426

G Length-to-maximum width ratio

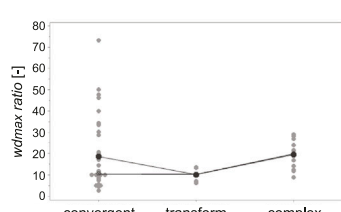


	N	min	mean	StDev	median	max
conv.	64	0,46	11,31	18,06	6,20	118,88
trans.	12	3,88	11,32	6,92	8,94	27,11
comp.	16	1,91	7,85	7,04	5,13	27,97

Welch's ANOVA
F-Value=2.33 DF Num=2 DF Den=28.0361 P-Value=0.116

	Dmean	SE	T-Value	adjusted P-Value
conv. vs trans.	0,1683	0,0904	1,86	0,172
conv. vs comp.	-0,0525	0,0991	-0,53	0,857
comp. vs trans.	-0,221	0,112	-1,97	0,140

H Maximum width-to-maximum depth ratio

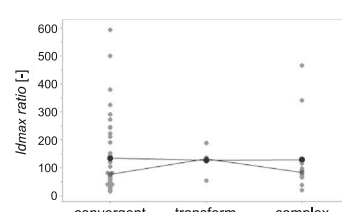


	N	min	mean	StDev	median	max
conv.	34	2,45	18,54	16,71	10,33	73,33
trans.	4	6,15	10,05	3,99	10,20	13,64
comp.	13	8,75	19,48	6,49	19,83	28,86

Welch's ANOVA
F-Value=4.53 DF Num=2 DF Den=9.57062 P-Value=0.041

	Dmean	SE	T-Value	adjusted P-Value
conv. vs trans.	-0,145	0,110	-1,32	0,434
conv. vs comp.	0,1451	0,0763	1,90	0,150
comp. vs trans.	0,290	0,101	2,87	0,083

I Length-to-maximum depth ratio



	N	min	mean	StDev	median	max
conv.	42	14,30	133,80	134,4	75,70	593,30
trans.	4	52,60	126,00	56,10	131,20	188,90
comp.	12	18,90	127,70	133,80	82,40	466,10

Welch's ANOVA
F-Value=0.47 DF Num=2 DF Den=9.60212 P-Value=0.641

	Dmean	SE	T-Value	adjusted P-Value
conv. vs trans.	0,136	0,137	1,00	0,609
conv. vs comp.	0,026	0,126	0,21	0,977
comp. vs trans.	-0,110	0,160	-0,69	0,776

FIGURE 4 | (A–I) Dot plots of morphometric values and aspect ratios for the studied canyons from active margins, classified on plate-boundary type. N, number of readings; min, minimum value; mean, mean value; SD, standard deviation; median, median value; max, maximum value. Results of Welch's ANOVA test: DF Num, degrees of freedom numerator; DF Den, degrees of freedom denominator. Games-Howell *post hoc* test: D_{mean}, difference of means; SE, standard error.

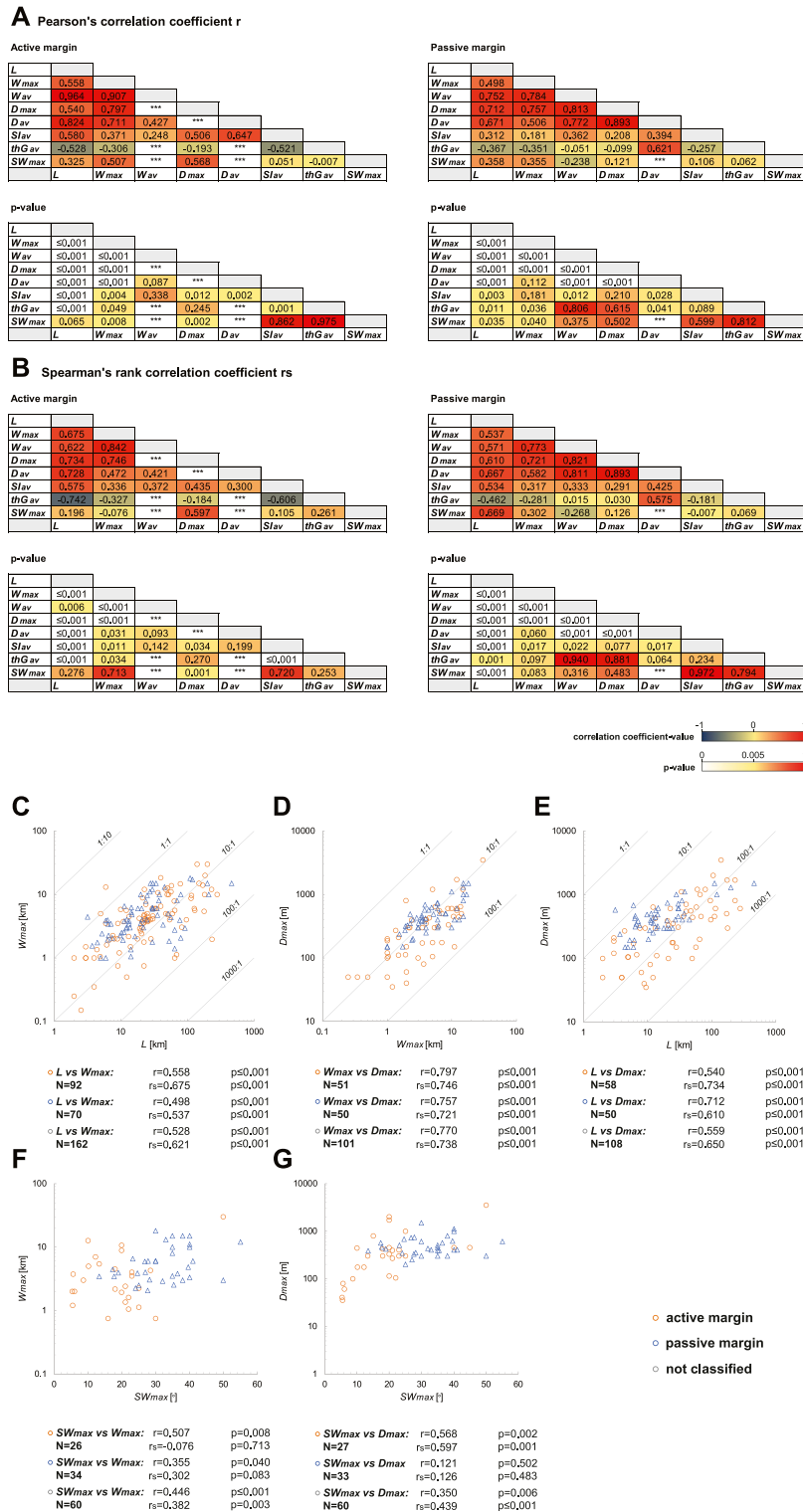


FIGURE 5 | (A–G) Results of the correlation analyses of canyon morphometric parameters with attributes of the physiographic setting at the canyon in active vs. passive margins. **(A,B)** Overview of results presented as heat maps. **(C–G)** Scatter plots of results. *L*, canyon length; *W_{max}*, maximum canyon width; *W_{av}*, average canyon width; *D_{max}*, maximum canyon depth; *D_{av}*, average canyon depth; *Sl_{av}*, average canyon sinuosity index; *thG_{av}*, average canyon thalweg gradient; *SW_{max}*, maximum canyon sidewall steepness; *N*, number of readings; *r*, Pearson's correlation coefficient; *r_s*, Spearman's rank correlation coefficient.

ANOVA and Games-Howell post-hoc tests, no significant differences are seen for average values across the different active-plate boundary types (Figure 4D).

Submarine canyons in complex settings exhibit a greater range in values of the average canyon thalweg gradient than those in convergent margins, but on average, the overall thalweg gradient is only 1.18 times steeper, and not significantly different (Figure 4E).

Canyons in convergent settings display a great range in maximum sidewall steepness, which is on average 20.3°. There exists insufficient data on margin steepness in canyons located in transform and complex settings to conduct meaningful analyses on these, but the data available demonstrate that canyons in these settings can reach gradients of 30.0° and 28.5°, respectively; these values are higher than those recorded in the majority of convergent-margin canyons (Figure 4F).

3.2 Scaling in Submarine Canyons in Active Versus Passive Margins

Results of the correlation analyses of canyon morphometric parameters with each other are presented as heat maps (Figures 5A,B). Additionally, correlations between maximum canyon dimensions and their aspect ratios (Figures 5C–E) and between maximum canyon sidewall steepness and maximum width (Figure 5F) and depth (Figure 5G) are also displayed as scatter plots.

3.2.1 Canyon Dimensions

Moderate and statistically significant scaling between maximum canyon dimensions is seen for submarine canyons along both active and passive margins (Figures 5A–E).

3.2.2 Maximum Canyon Sidewall Steepness vs. Maximum Canyon Width and Depth

A moderate linear correlation is seen between maximum sidewall steepness and maximum width in active-margin canyons, whereas the same parameters are weakly correlated in passive-margin canyons (Figure 5F).

Correlations of maximum sidewall steepness with maximum depth (Figure 5G) are weak and not significant for passive-margin examples. In contrast, maximum sidewall steepness displays moderate correlations with maximum depth in canyons along active margins, which are statistically significant.

3.3 Scaling Between Canyon Morphometric Parameters and Characteristics of Their Physiographic Setting in Active Versus Passive Margins

Results of the correlation analyses of canyon morphometric apex (Section 3.3.1) and mouth, and with the distance of the canyon to the nearest shoreline (Section 3.3.2) are presented as heat maps (Figures 6A,B). In addition, discussed scaling relationships are presented as scatter plots (Figures 7A–H).

3.3.1 Seafloor Depth at the Canyon Apex

In canyons from active and passive margins, the seafloor depth at the canyon apex correlates weakly with canyon length, maximum canyon width and average canyon thalweg gradient (Figures 6A,B). For average canyon width and seafloor depth at the canyon apex, moderate to modest negative correlations are seen in both active and passive margins, which are only significant for the latter (Figure 7A). A negative and significant moderate correlation between seafloor depth and maximum canyon depth is seen for passive-margin canyons; the corresponding relationship is instead weak for canyons along active margins (Figure 7B). Average canyon depth displays negative and modest correlations with the seafloor depth at the canyon apex along passive margins, but these are not significant for the chosen alpha value (Figure 7C).

Moderate inverse relationships between seafloor depth and both average canyon sinuosity (Figure 7D) and maximum canyon sidewall steepness (Figure 7E) exist in active margins, which are statistically significant. For canyons in passive margins, the correlations with apex depth are weak for both morphometric parameters (Figures 7D,E).

For the investigated aspect ratios, significant and moderate positive scaling exists with $w_{d,max}$ ratios of canyons in active settings (Figure 7F). The remaining correlations in both margin types are all weak (Figures 6A,B).

3.3.2 Minimum Canyon-Shoreline Distance

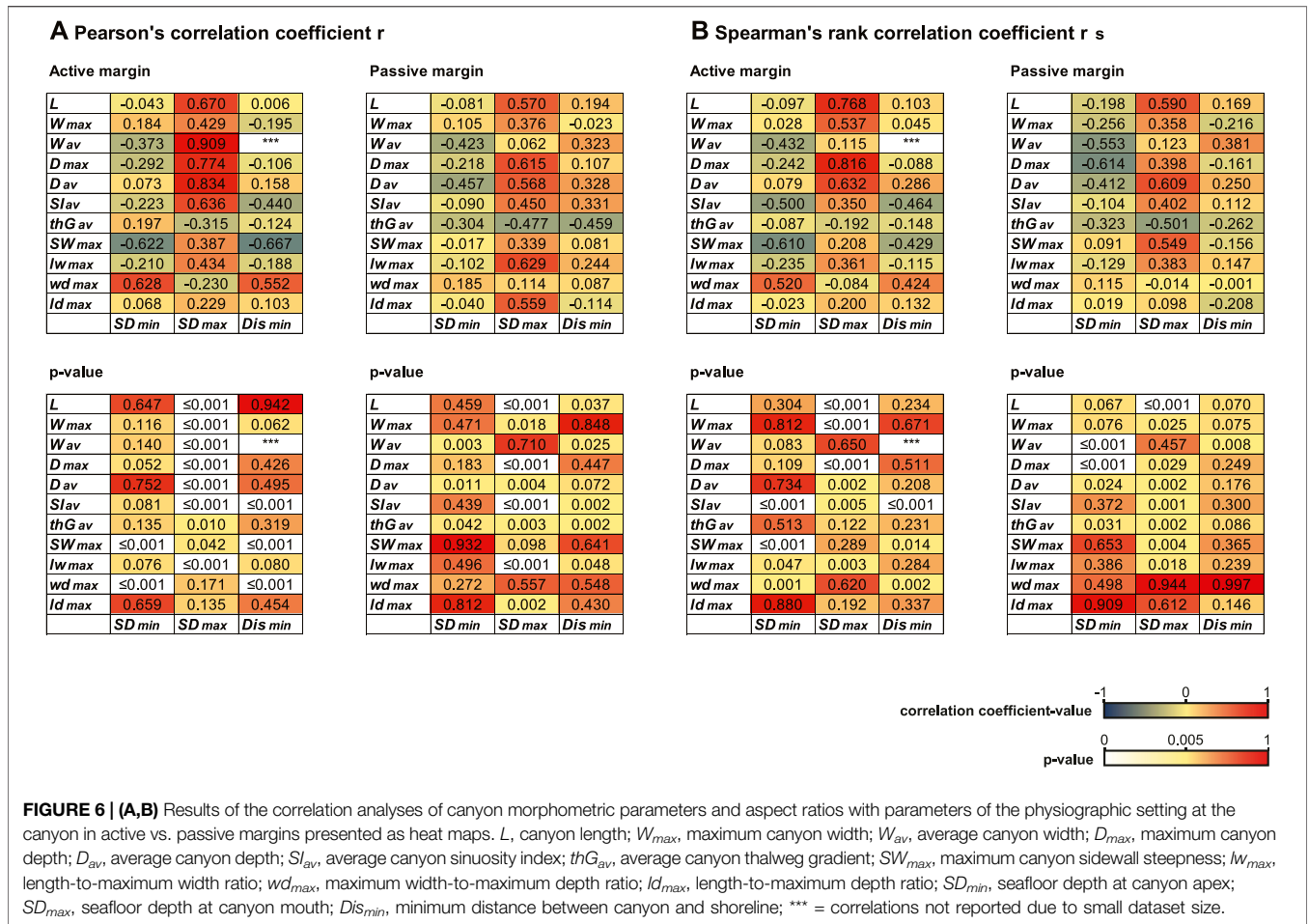
Correlations between the shortest distance of the canyon to the shoreline with canyon morphometric parameters are weak for all maximum and average canyon dimensions for canyons from both margin types. Relationships with average canyon width in active-margin canyons were not assessed due to insufficient data for the statistical analyses (Figures 6A,B).

Average canyon sinuosity demonstrates modest negative scaling with the minimum distance of the canyon to the shoreline in active margins, whereas weak positive scaling is seen for passive margins; correlations are statistically significant for both margins (Figures 6A,B).

Inverse scaling between the minimum canyon-shoreline distance and the average canyon thalweg gradient is seen in canyons from both margin types. The correlation is weak for examples from active margins, whereas modest, linear negative correlation is seen for passive-margin settings (Figures 6A,B).

With decreasing distance of the canyon to the coastline, the maximum sidewall steepness in active-margin canyons tends to increase, but the strength of this correlation is moderate to modest. Correlation between the two parameters is very weak in examples from passive margins (Figure 7G).

Correlations of aspect ratios with minimum distance to the shoreline are weak for maximum canyon dimensions across both margin types (Figures 6A,B), with the exception of significant moderate and modest scaling displayed for $w_{d,max}$ ratios in active-margin canyons (Figure 7H).



3.4 Scaling Between Canyon Morphometry and Characteristics of the Source-to-Sink System

Scaling relationships between canyon morphometric parameters and attributes of the terrestrial catchment (Figures 8A–L), shelf (Figures 8M–Q, 9A) and slope (Figures 8R, 9B) have been assessed.

3.4.1 Terrestrial Catchment (Fluvial System Length, Average Annual Fluvial Water Discharge, Catchment Size, Maximum Catchment Elevation)

For the studied canyons with a present and/or past sediment connection with one or several fluvial systems, scaling of canyon length and average canyon sinuosity with attributes of the terrestrial catchment in active and passive margins can be quantified. Statistical analyses on maximum canyon width are limited to active-margin settings in view of data coverage.

3.4.1.1 Fluvial System Length

Correlations of river length with canyon length are weak and not significant for canyons in passive margins. Along active margins, positive and moderate scaling of canyon length with fluvial

system length is demonstrated, which is statistically significant (Figure 8A). In contrast, maximum width correlates weakly with river length in canyons along active margins, but relatively strongly for canyons located in passive-margin settings. However, findings for the latter group are based on thirteen observations only (Figure 8E). For average canyon sinuosity, the correlations are weak and not significant for any margin type (Figure 8I).

3.4.1.2 Average Annual Fluvial Water Discharge

The average annual water discharge of the fluvial system displays positive, moderate monotonic correlations with canyon length in canyons of both margin types, as well as overall in the entire dataset; these relationships are statistically significant (Figure 8B). Correlations of average annual fluvial discharge and maximum width are weak in active-margin canyons (Figure 8F). Positive and monotonic correlations of average canyon sinuosity with this catchment attribute exist for active and passive margins, but these are respectively moderate and weak, and neither is statistically significant (Figure 8J).

3.4.1.3 Catchment Size

Scaling of canyon length with catchment size is weak for canyons from passive margins (Figure 8C). Moderate, positive monotonic

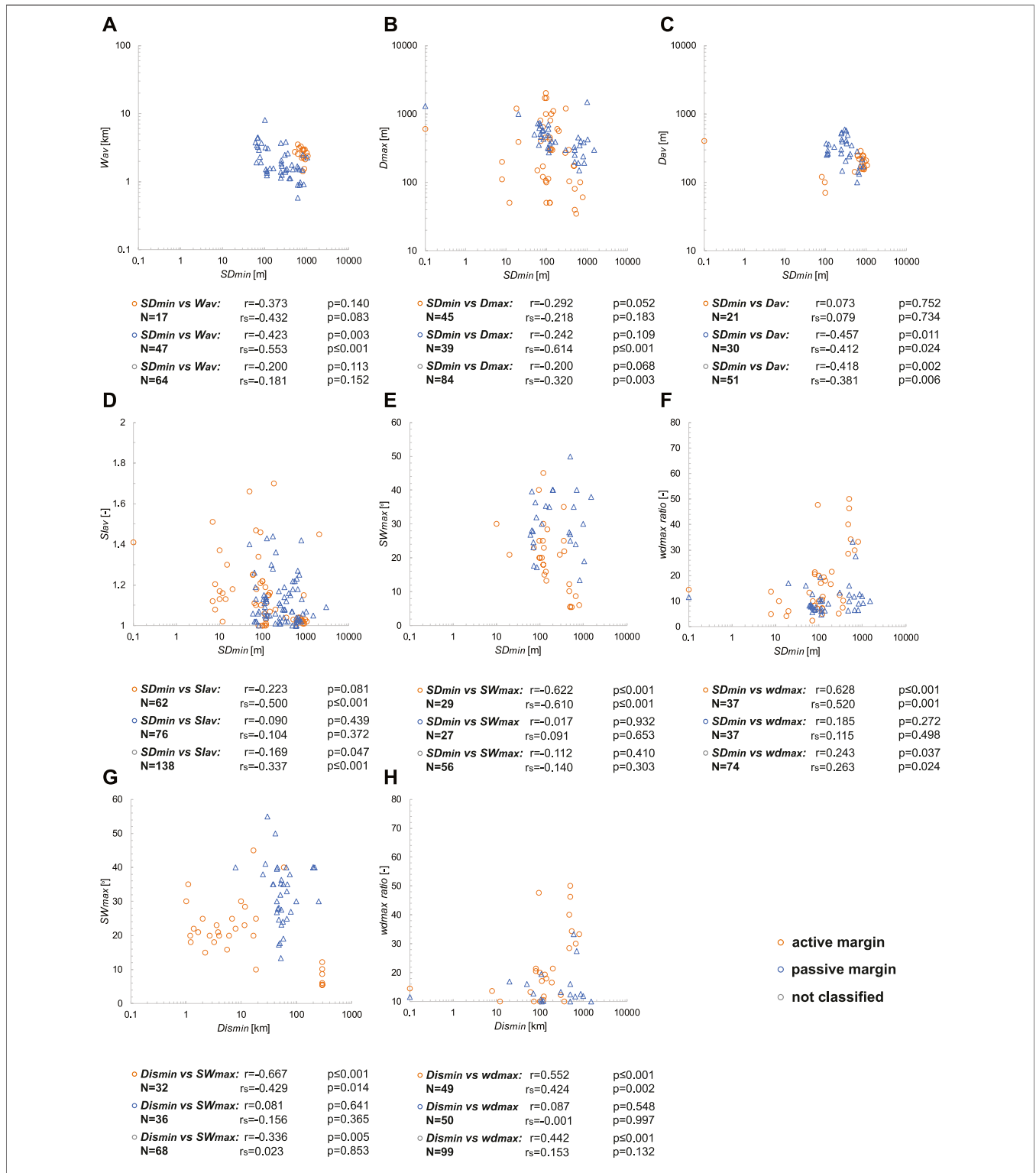


FIGURE 7 | (A–H) Scatterplots of attributes of the canyon-physiographic setting with canyon morphometric parameters for submarine canyons of the study in active vs. passive margins. W_{av} , average canyon width; D_{max} , maximum canyon depth; D_{av} , average canyon depth; Sl_{av} , average canyon sinuosity index; SW_{max} , maximum canyon sidewall steepness; wd_{max} ratio, maximum width-to-maximum depth ratio; SD_{min} , minimum water depth at the canyon apex; Dis_{min} , minimum canyon distance to the shoreline; N , number of readings; r , Pearson's correlation coefficient; r_s , Spearman's rank correlation coefficient.

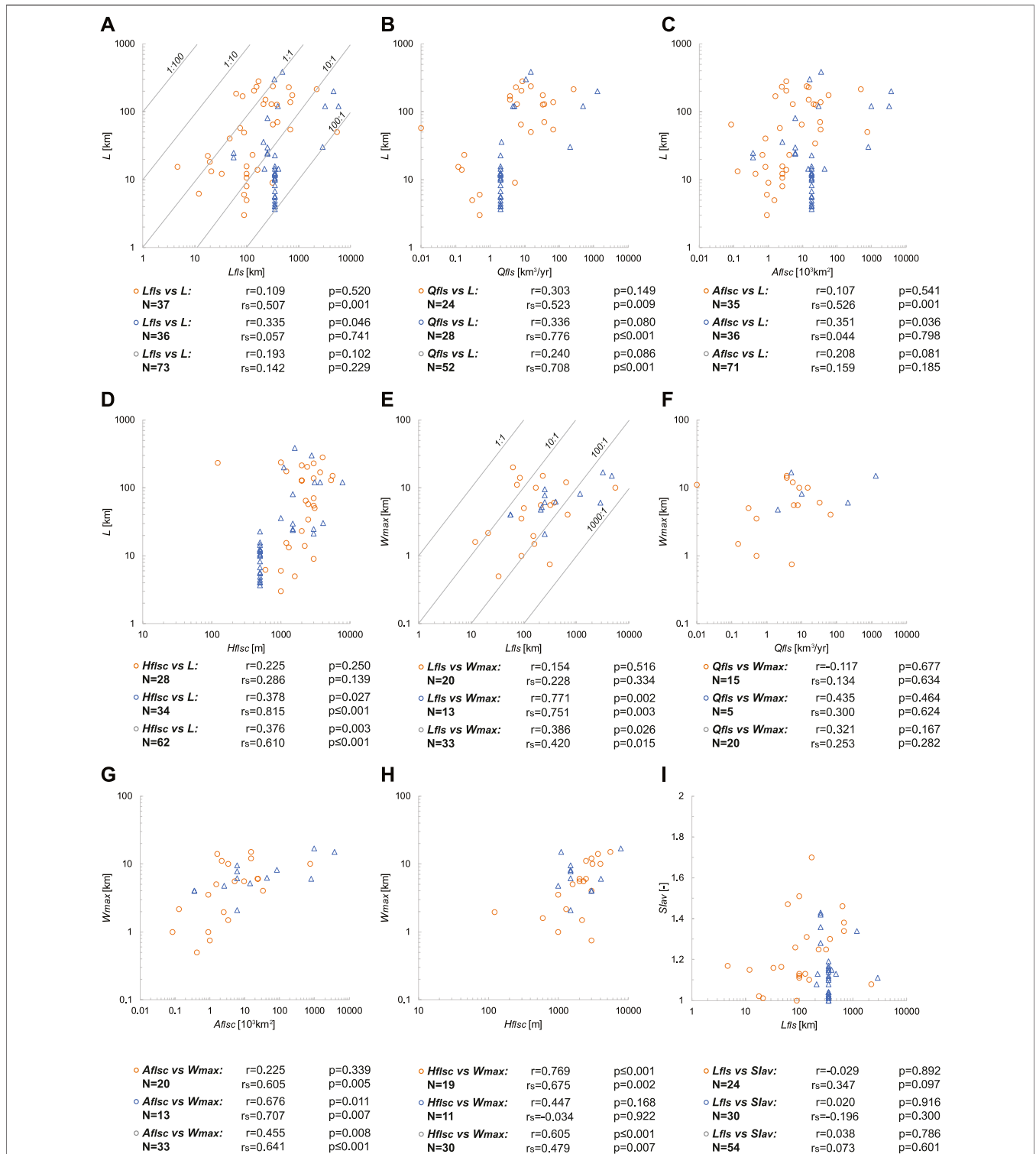
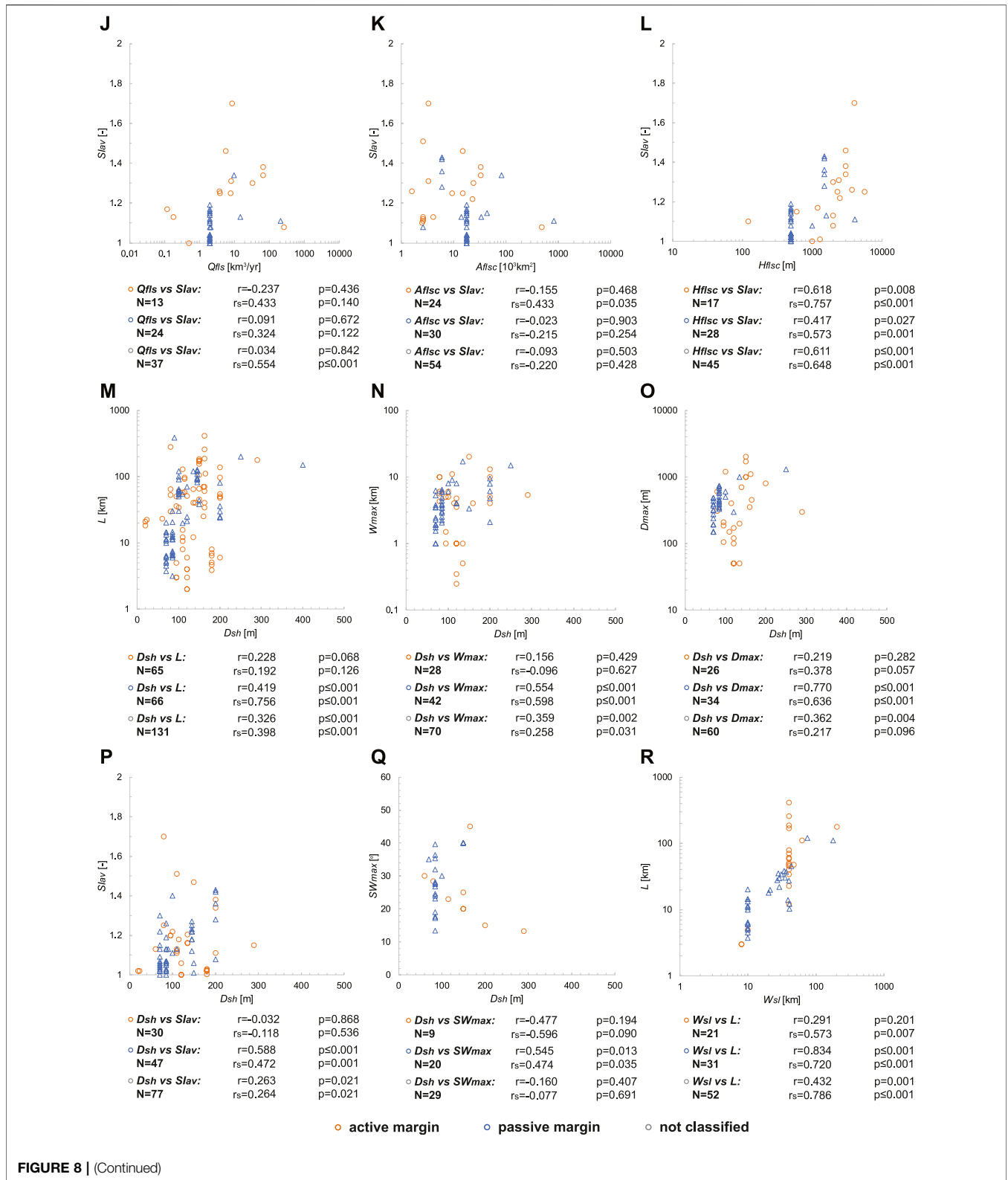


FIGURE 8 | (A–I) Scatterplots of attributes of the terrestrial catchment, shelf and slope with canyon morphometric parameters for submarine canyons of the study in active vs. passive margins. L , canyon length; W_{max} , maximum canyon width; S_{lav} , average canyon sinuosity index; SW_{max} , maximum canyon sidewall steepness; L_{fsc} , fluvial system length; Q_{fsc} , average annual fluvial discharge; A_{fsc} , catchment size; H_{fsc} , Maximum catchment elevation; D_{sh} , shelf-break depth; W_{sh} , slope width. N , number of readings; r , Pearson's correlation coefficient; r_s , Spearman's rank correlation coefficient.



correlations exist for the length (**Figure 8C**) and maximum width (**Figure 8G**) in canyons associated with active margins. No correlation is seen between average canyon sinuosity and

catchment area for passive-margin canyons; a modest, positive monotonic correlation is seen for active-margin settings, but this is not significant (**Figure 8K**).

A Shelf

Pearson's correlation coefficient r

Active margin

L	0.227	0.228	-0.414
W _{max}	0.066	0.156	-0.422
D _{max}	0.227	0.219	-0.407
Sl _{av}	-0.368	-0.032	0.029
thG _{av}	-0.179	0.210	0.180
SW _{max}	0.373	-0.477	-0.418
lw _{max}	-0.188	0.207	0.059
wd _{max}	-0.033	-0.066	-0.095
ld _{max}	-0.101	0.404	-0.092
	W _{sh}	D _{sh}	G _{sh}

Passive margin

L	0.245	0.419	0.083
W _{max}	0.133	0.554	0.283
D _{max}	0.198	0.770	-0.193
Sl _{av}	0.260	0.588	0.645
thG _{av}	-0.490	-0.343	-0.178
SW _{max}	0.533	0.545	-0.466
lw _{max}	0.267	0.515	0.490
wd _{max}	0.413	0.285	-0.481
ld _{max}	0.059	0.838	-0.674
	W _{sh}	D _{sh}	G _{sh}

Spearman's rank correlation coefficient rs

Active margin

L	0.365	0.192	-0.537
W _{max}	0.339	-0.096	0.283
D _{max}	0.525	0.378	-0.525
Sl _{av}	-0.344	-0.118	0.089
thG _{av}	-0.339	0.238	0.298
SW _{max}	0.288	-0.596	-0.370
lw _{max}	0.013	0.165	-0.086
wd _{max}	0.093	-0.100	-0.196
ld _{max}	0.270	0.236	-0.171
	W _{sh}	D _{sh}	G _{sh}

Passive margin

L	0.356	0.756	-0.168
W _{max}	-0.052	0.598	0.192
D _{max}	0.202	0.636	0.205
Sl _{av}	0.049	0.472	0.036
thG _{av}	-0.302	-0.311	0.200
SW _{max}	0.322	0.474	-0.333
lw _{max}	0.325	0.377	-0.139
wd _{max}	0.105	0.234	-0.304
ld _{max}	-0.080	0.041	-0.281
	W _{sh}	D _{sh}	G _{sh}

p-value

L	0.014	0.068	0.001
W _{max}	0.572	0.429	0.025
D _{max}	0.149	0.282	0.035
Sl _{av}	0.001	0.868	0.880
thG _{av}	0.153	0.171	0.242
SW _{max}	0.087	0.194	0.263
lw _{max}	0.115	0.299	0.769
wd _{max}	0.857	0.796	0.689
ld _{max}	0.535	0.045	0.655
	W _{sh}	D _{sh}	G _{sh}

p-value

L	0.016	≤0.001	0.521
W _{max}	0.353	≤0.001	0.073
D _{max}	0.240	≤0.001	0.281
Sl _{av}	0.022	≤0.001	≤0.001
thG _{av}	0.001	0.028	0.265
SW _{max}	0.013	0.013	0.039
lw _{max}	0.066	0.001	0.002
wd _{max}	0.014	0.107	0.005
ld _{max}	0.735	≤0.001	≤0.001
	W _{sh}	D _{sh}	G _{sh}

p-value

L	≤0.001	0.126	≤0.001
W _{max}	0.003	0.627	0.073
D _{max}	≤0.001	0.057	0.005
Sl _{av}	0.002	0.536	0.640
thG _{av}	0.006	0.119	0.050
SW _{max}	0.193	0.090	0.327
lw _{max}	0.913	0.409	0.671
wd _{max}	0.606	0.692	0.408
ld _{max}	0.092	0.256	0.403
	W _{sh}	D _{sh}	G _{sh}

p-value

L	≤0.001	≤0.001	0.192
W _{max}	0.715	≤0.001	0.228
D _{max}	0.231	≤0.001	0.252
Sl _{av}	0.670	0.001	0.810
thG _{av}	0.044	0.047	0.209
SW _{max}	0.154	0.035	0.152
lw _{max}	0.024	0.016	0.405
wd _{max}	0.550	0.190	0.091
ld _{max}	0.647	0.819	0.119
	W _{sh}	D _{sh}	G _{sh}

B Slope

Pearson's correlation coefficient r

Active margin

L	0.291	0.305	0.221
W _{max}	0.018	0.342	0.289
D _{max}	-0.034	0.655	0.566
Sl _{av}	***	0.244	0.201
thG _{av}	-0.262	-0.066	-0.018
SW _{max}	***	0.222	0.424
lw _{max}	0.970	0.438	-0.085
wd _{max}	-0.038	-0.203	-0.647
ld _{max}	0.960	0.282	-0.530
	W _{sl}	D _{sl}	G _{sl}

Passive margin

L	0.834	-0.034	-0.327
W _{max}	0.639	-0.428	-0.707
D _{max}	0.730	0.150	-0.740
Sl _{av}	-0.383	0.328	-0.308
thG _{av}	-0.341	0.279	0.638
SW _{max}	-0.271	-0.344	0.149
lw _{max}	0.333	0.490	0.089
wd _{max}	0.170	-0.183	-0.381
ld _{max}	0.512	0.259	-0.690
	W _{sl}	D _{sl}	G _{sl}

Spearman's rank correlation coefficient rs

Active margin

L	0.573	0.381	0.309
W _{max}	0.236	0.244	0.319
D _{max}	0.285	0.535	0.652
Sl _{av}	***	0.170	0.423
thG _{av}	-0.171	0.161	0.044
SW _{max}	***	0.118	0.725
lw _{max}	0.736	0.402	-0.091
wd _{max}	0.204	-0.082	-0.675
ld _{max}	0.801	0.214	-0.644
	W _{sl}	D _{sl}	G _{sl}

Passive margin

L	0.720	0.152	-0.578
W _{max}	0.671	-0.372	-0.700
D _{max}	0.446	0.111	-0.553
Sl _{av}	-0.420	0.344	-0.325
thG _{av}	-0.397	0.295	0.742
SW _{max}	-0.402	-0.598	0.020
lw _{max}	0.153	0.486	0.017
wd _{max}	0.564	-0.129	-0.569
ld _{max}	0.736	0.533	-0.707
	W _{sl}	D _{sl}	G _{sl}

p-value

L	0.201	0.005	0.166
W _{max}	0.956	0.016	0.152
D _{max}	0.911	≤0.001	0.004
Sl _{av}	***	0.157	0.511
thG _{av}	0.278	0.623	0.930
SW _{max}	***	0.360	0.170
lw _{max}	≤0.001	0.003	0.686
wd _{max}	0.912	0.256	0.002
ld _{max}	≤0.001	0.091	0.009
	W _{sl}	D _{sl}	G _{sl}

p-value

L	≤0.001	0.788	0.030
W _{max}	≤0.001	0.005	≤0.001
D _{max}	≤0.001	0.517	≤0.001
Sl _{av}	0.087	0.036	0.081
thG _{av}	0.278	0.209	0.001
SW _{max}	0.293	0.149	0.567
lw _{max}	0.072	0.002	0.626
wd _{max}	0.368	0.441	0.038
ld _{max}	0.003	0.284	≤0.001
	W _{sl}	D _{sl}	G _{sl}

p-value

L	0.007	≤0.001	0.049
W _{max}	0.460	0.091	0.112
D _{max}	0.346	≤0.001	0.001
Sl _{av}	***	0.329	0.150
thG _{av}	0.484	0.227	0.831
SW _{max}	***	0.629	0.008
lw _{max}	0.010	0.006	0.666
wd _{max}	0.548	0.650	0.001
ld _{max}	0.002	0.203	0.001
	W _{sl}	D _{sl}	G _{sl}

p-value

L	≤0.001	0.228	≤0.001
W _{max}	≤0.001	0.017	≤0.001
D _{max}	0.012	0.632	0.001
Sl _{av}	0.058	0.028	0.065
thG _{av}	0.202	0.183	≤0.001
SW _{max}	0.109	0.007	0.938
lw _{max}	0.419	0.002	0.928
wd _{max}	0.001	0.588	0.001
ld _{max}	≤0.001	0.019	≤0.001
	W _{sl}	D _{sl}	G _{sl}

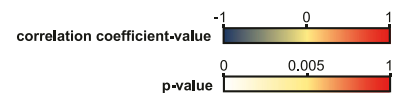


FIGURE 9 | (A,B) Results of the correlation analyses of canyon morphometric parameters with attributes of the **(A)** shelf and **(B)** slope at the canyon in active vs. passive margins presented as heat maps. L, canyon length; W_{max}, maximum canyon width; D_{max}, maximum canyon depth; Sl_{av}, average canyon sinuosity index; thG_{av}, average canyon thalweg gradient; SW_{max}, maximum canyon sidewall steepness; lw_{max}, length-to-maximum width ratio; wd_{max}, maximum width-to-maximum depth ratio; ld_{max}, length-to-maximum depth ratio; W_{sh}, shelf width; D_{sh}, shelf-break depth; G_{sh}, average shelf gradient; W_{sl}, slope width; D_{sl}, slope-break depth; G_{sl}, average slope gradient; *** = correlations not reported due to small dataset size.

3.4.1.4 Maximum Catchment Elevation

The length of submarine canyons scales positively with the maximum catchment elevation of associated fluvial systems on passive margins. A corresponding relationship is absent for active

margins (Figure 8D), whereas maximum canyon width shares positive and moderate correlations with maximum catchment elevation in active-margin canyons (Figure 8H). Moderate, significant correlations are seen between average canyon

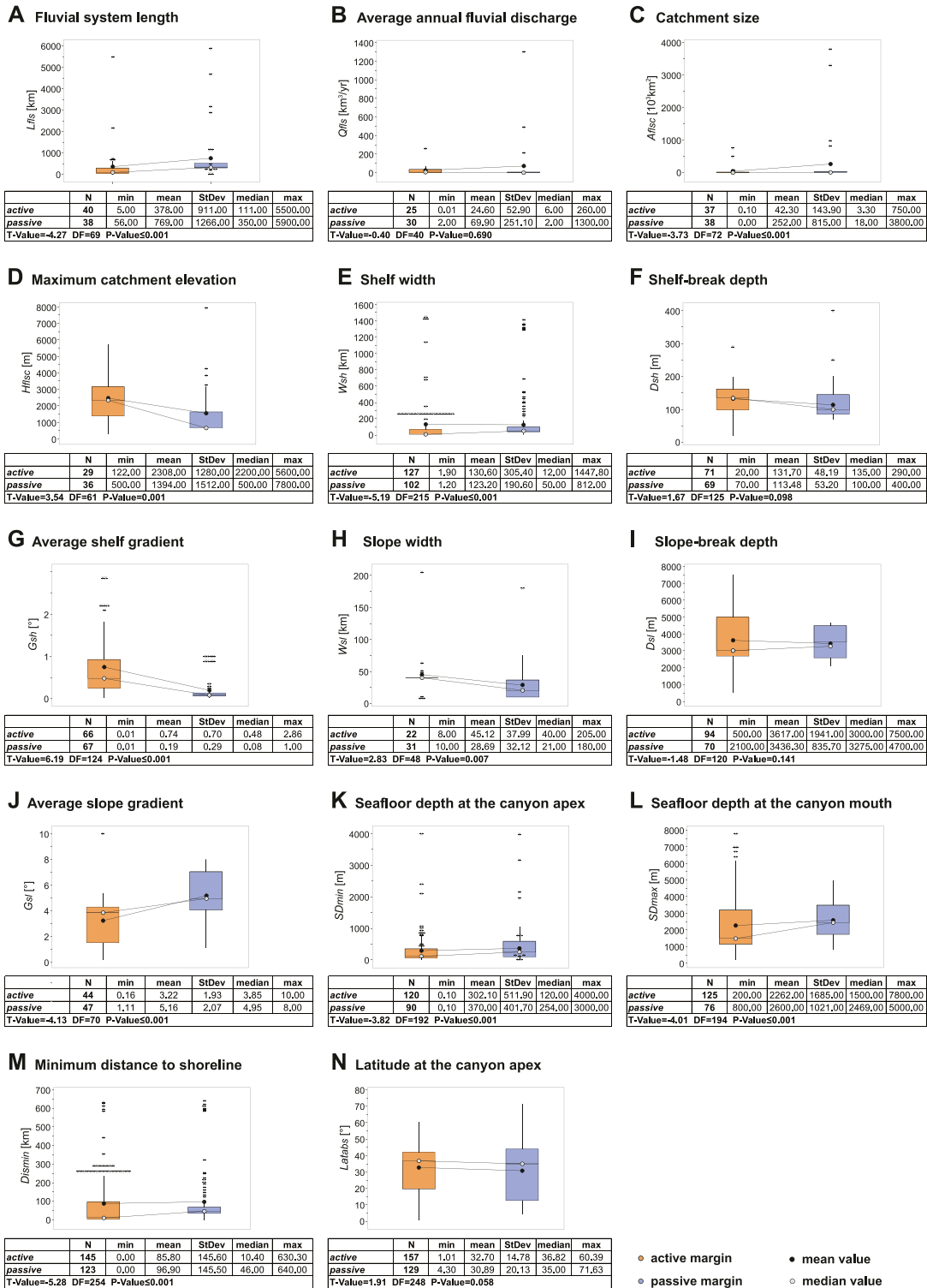


FIGURE 10 | (A–N) Boxplots of frequency distributions of attributes of source-to-sink systems and of the canyon-physiographic setting linked to submarine canyons of active and passive margins. *N*, number of readings; min, minimum value; mean, mean value; SD, standard deviation; median, median value; max, maximum value; DF, degrees of freedom.

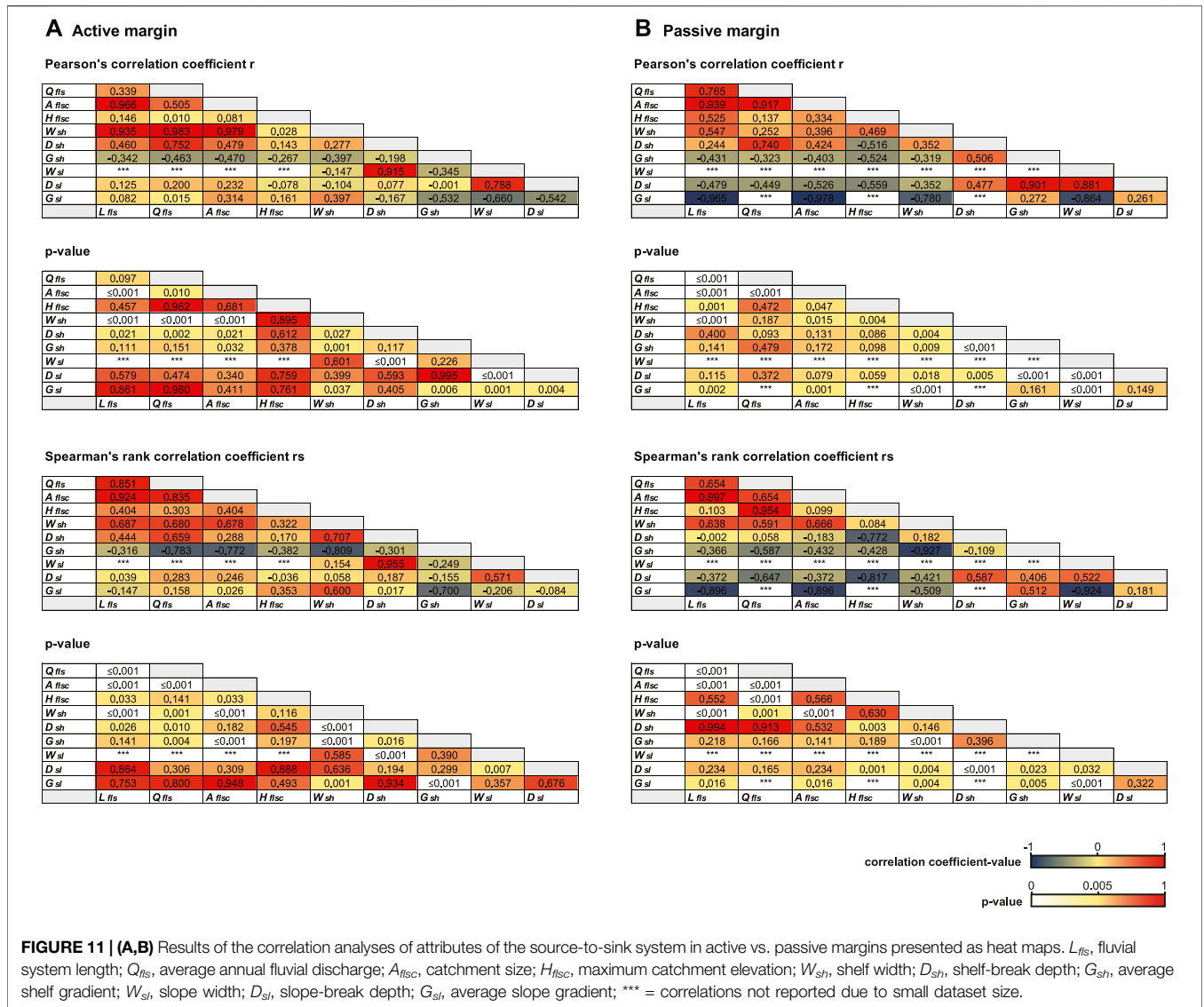


FIGURE 11 | (A,B) Results of the correlation analyses of attributes of the source-to-sink system in active vs. passive margins presented as heat maps. L_{fls} , fluvial system length; Q_{fls} , average annual fluvial discharge; A_{fisc} , catchment size; H_{fisc} , maximum catchment elevation; W_{sh} , shelf width; D_{sh} , shelf-break depth; G_{sh} , average shelf gradient; W_{sl} , slope width; D_{sl} , slope-break depth; G_{sl} , average slope gradient; *** = correlations not reported due to small dataset size.

sinuosity and maximum catchment elevation for both margin types (Figure 8L).

3.4.2 Shelf-Break Depth

Correlations of shelf-break depth at the canyon location with attributes of canyon geomorphology are weak and not significant for canyons in active-margin settings; in the studied canyons from passive margins, instead, maximum canyon dimensions (Figures 8M–O), average canyon sinuosity (Figure 8P) and maximum canyon sidewall steepness (Figure 8Q) correlate moderately or strongly with the shelf-break depth (Figure 9A).

3.4.3 Slope Width

Canyon length increases with slope width in active and passive margins; the strength of the relationship is moderate in the former and strong in the latter (Figure 8R). Maximum canyon width and depth do not correlate with the slope width in active margins, but both variables show moderate correlation with the width of

passive-margin slopes. However, more data are needed to support the findings for active-margin canyons (Figure 9B).

3.5 Characterization of Canyon Source-to-Sink System and Physiographic Setting by Tectonic Setting

Analyses have been undertaken of 1) attributes of the S2S system and of the physiographic setting, and of how these vary with the margin type (Section 3.5.1), and of 2) scaling between attributes of the S2S systems in active and passive margins (Section 3.5.2). This has been done for the following reasons: 1) to assess commonalities and differences in characteristics of the two margin types, which can be used to refine existing S2S system models; and 2) to aid recognition of covariance between variables that may be related to the studied canyon morphometric parameters, rendered necessary by data gaps that prevent the application of multivariate techniques.

3.5.1 Attributes of the Canyon Geological Contexts and Their Variations Across Margin Types

Two-sample t-tests undertaken on frequency distributions of the attributes describing canyon terrestrial catchments, continental shelves and slopes (Figures 10A–N) demonstrate that significant differences in mean values of the studied variables are seen for all investigated attributes except for average annual fluvial discharge (Figure 10B), shelf-break depth (Figure 10F), slope-break depth (Figure 10I) and latitude at the canyon apex (Figure 10N).

On average, the length (Figure 10A), average annual water discharge (Figure 10B) and catchment size (Figure 10C) of fluvial systems supplying sediment to the studied canyons are each greater in terrestrial catchments along passive margins. Although the greatest maximum catchment elevation recorded in the study occurs in a passive-margin drainage basin, terrestrial catchments associated with active margins tend to be higher than along passive margins (Figure 10D).

The widest continental shelves in the study are associated with the submarine canyons of the Bering Sea, but the mean shelf widths of the studied active and passive margins are very similar, albeit slightly greater along the former (Figure 10E). Shelf-breaks tend to be deeper along active margins, but the results do not indicate a significant difference between the two margin types (Figure 10F). The average shelf gradient is on average higher in active-margin systems (Figure 10G).

Canyons of the study along active margins are hosted on wider (Figure 10H) and deeper (Figure 10I) slopes, whereas the average slope gradient tends to be higher in S2S systems associated with the studied passive margins (Figure 10J).

With regard to aspects of the physiographic setting, mean values of seafloor depth at the canyon apex and mouth, of the minimum distance of the canyon to the shoreline, and of the latitude of the canyon apex are similar across the two margin types. Active-margin canyons show a greater bathymetric range, and several of the studied canyons in passive margins are located at higher latitudes (Figures 10K–N).

3.5.2 Scaling Between Attributes of the Source-to-Sink Systems of Active and Passive Margins

Correlations between attributes of the terrestrial catchment, shelf and slope in canyon-associated S2S systems grouped into active- and passive-margin settings share similarities, yet exhibit differences regarding their sign, strength and statistical significance. For some attributes, the amount of data prevents meaningful analyses to be undertaken (Figures 11A,B).

Statistically significant scaling relationships are seen across both margin types, but these vary in strength. Strong and positive significant correlations of catchment area with fluvial-system length and average annual fluvial discharge are seen for both margin types. Also, shelf width correlates positively with catchment area and fluvial system length in both margin types, but the relationship with the latter is stronger in active-margin settings. Strong inverse scaling across both margin types exists between shelf width and the average shelf gradient and between slope width and the average slope gradient in passive margins (Figures 11A,B).

For other pairs of attributes, significant relationships may be seen for a particular margin type only. For example, the maximum elevation of passive-margin catchments shows significant and positive scaling with fluvial system length and average annual fluvial discharge, which is moderate for the former and strong for the latter. For active margins, correlations are weak and modest and not statistically significant. Shelf-break depth and the average shelf gradient display linear, moderate and significant positive correlation with each other in passive margins, but along active margins the same trend is weak, negative and not statistically significant (Figures 11A,B).

4 DISCUSSION

4.1 Tectonic Influence on Controlling Factors on Submarine-Canyon Geomorphology

Findings from this study suggest that certain aspects of the morphometry of submarine canyons, and some scaling relationships of canyon morphometric parameters mutually and with attributes of their geological setting, are more strongly expressed in a specific margin type (see Figures 2–9), indicating a possible tectonic control. Although commonalities seen in scaling across both margin types indicate that a scaling relationship might not be generally sensitive to factors related to tectonic activity, the possibility exists that tectonic influences might be overridden by other controlling factors or that different controls in passive and active margins have led to similar geomorphologic expressions in canyons.

In the following sections, the main findings of the study are discussed in the context of a potential tectonic influence on controlling factors on submarine-canyon geomorphology, including intra-canyon sedimentary processes, sediment connection to fluvial and littoral sources, sediment supply to shelf margins and structural controls.

4.1.1 Intra-Canyon Sedimentary Processes

The contrast in relative importance of intra-canyon processes along active and passive margins may contribute to certain differences seen in scaling relationships between canyons of the two margin types. For example, intra-canyon-wall failure might be less important as a geomorphic agent in canyons from active margins compared to passive-margin ones (Bührig et al., in review). This is because slope failures are thought to occur less commonly along active margins compared to passive margins, due to strengthening of the seafloor from recurrent seismic activity (e.g., Strozyk et al., 2010; Nelson et al., 2011; Sawyer and DeVore, 2015; Molenaar et al., 2019); on active margins, large-scale slope failures tend to be linked to high-magnitude earthquakes (e.g., Strozyk et al., 2010; Molenaar et al., 2019). By contrast, active-margin settings with steep terrestrial catchments and narrow and steep shelf configurations promote maintenance of sediment connection of submarine canyons with fluvial outlets and littoral cells even during periods of sea-level highstand, as at

present (e.g., Gamberi et al., 2015; Bernhardt and Schwanghart, 2021). Hence, moderate correlations of maximum sidewall steepness with maximum canyon width (**Figure 5F**) and depth (**Figure 5G**) in canyons along active margins might reflect the tendency of sediment gravity flows to predominate over intra-canyon slope failure in shaping canyon geomorphology in these settings, *via* their ability to concurrently control canyon width, depth and bank steepness by thalweg erosion (e.g., McHargue et al., 2011; Peakall and Sumner, 2015) and canyon margin aggradation from flow overspilling (e.g., Armitage et al., 2010; Soulet et al., 2016). In contrast, the weaker correlations seen for passive-margin canyons (**Figures 5F,G**) may be linked to the combined effect of a subordinate influence of sediment gravity flows from the disconnection of canyons to fluvial and intrashelf sources during periods of sea-level highstand (e.g., Harris and Whiteway, 2011), paired with the variable impact of canyon-wall failure on canyon-wall slopes, canyon width and canyon depth. As a result, relationships between these morphometrics linked to intracanyon erosion by flows might be overprinted. When deposited near their source, mass failures and their depositional products will lead to lower canyon depths and greater canyon-floor widths over the affected areas, whereas the maximum width between the canyon banks will only increase where the wall collapse extends to the uppermost canyon margin. Intra-canyon slope failures may also have an indirect effect on canyon geomorphology away from the site of failure, particularly when the mass failure transitions into a sediment gravity flow (e.g., Stow, 1986; Hsu et al., 2008), or when the deposit is remobilized at a later point in time and is transported down canyon (e.g., Khrifounoff et al., 2012); as a consequence, mass-failure impact on canyon width, depth and sidewall gradients might vary.

Thus, the co-occurrence of wall failure and sediment gravity flows, which is recognized to act as an autogenic control on the variability in width-to-depth ratios of submarine channels (see **Figure 11** and text in Shumaker et al., 2018), may also be effective in controlling maximum width-to-maximum depth ($w_{d_{max}}$) ratios of submarine canyons (Bührig et al., in review). The smaller mean value and range of $w_{d_{max}}$ ratio seen for passive-margin canyons compared to active-margin ones (**Figures 3B, 5D**) suggest that width-to-depth aspect ratios in canyons hosted on passive margins tend to be constrained in their magnitude by the way in which wall-collapse may limit canyon-margin aggradation. By contrast, the subordinate role of intra-canyon failure combined with the effect of structural controls on canyon depths and widths (see **Section 4.1.4**) can explain the greater range in $w_{d_{max}}$ ratios seen in active-margin canyons (**Figures 3B, 5D**).

4.1.2 Sediment Connection to Fluvial and Littoral Sources

4.1.2.1 Sediment Discharge From Rivers

Some geomorphic features of submarine canyons are seen to scale, to some degree, with fluvial system length, average annual water discharge, catchment size and maximum catchment elevation. These observations are interpreted to reflect the importance of sediment discharge from rivers as controls on

how canyon geomorphology is shaped by erosional and depositional processes (cf. Casalbore et al., 2011; Bührig et al., in review).

For submarine canyons in active margins, potential causal links between fluvial sediment supply and their length and maximum width are suggested by: 1) moderate scaling of the former with fluvial system length (**Figure 8A**), average annual water discharge (**Figure 8B**) and catchment size (**Figure 8C**), and 2) moderate scaling of the latter with the area (**Figure 8G**) and maximum elevation (**Figure 8H**) of the associated terrestrial catchment. These relationships probably reflect how erosive intracanyon flows related to fluvial discharge promote lengthening at the canyon head (e.g., Piper and Normark, 2009) and mouth (e.g., Hodgson et al., 2016), as well as canyon widening (e.g., Casalbore et al., 2011).

By contrast, weak correlations of passive-margin canyon length with fluvial system length (**Figure 8A**) and catchment size (**Figure 8C**) indicate a lack of control of sediment discharge from rivers on canyon length. This might in part reflect how retrogressive slope failure tends to be a more prominent process along passive margins compared to active ones, and how sediment connection of canyons with fluvial sources in passive-margin settings tend to diminish through time at times of marine transgression (see **Section 4.1.1**). For example, incised valleys along passive margins are thought to be more prone to infill during transgressive and highstand intervals due to their commonly shallower depths compared to those along active margins, promoting the disconnection of canyon heads from fluvial sediment sources in passive-margin settings (Harris and Whiteway, 2011). Also, flooding events are less likely to trigger hyperpycnal flows at the mouth of rivers along passive margins, due to the increased sand-grade sediment segregation in their larger coastal and alluvial floodplains (e.g., Milliman and Syvitski, 1992; Sømme et al., 2009). In addition, larger terrestrial catchments are less affected by extreme weather events, in proportion to their size, compared to smaller ones (e.g., Sømme et al., 2009; Reid and Frostick, 2011).

Despite this, comparably strong scaling of canyon length with average annual fluvial discharge for passive-margin canyons (**Figure 8B**) might reflect that long-lived sediment-laden turbulent flows (*sensu* Zavala, 2020) linked to discharge from rivers are efficient in traversing wide shelves and entire canyons even during periods of sea-level highstand, and are effective in increasing canyon lengths by erosion at the canyon head and at its mouth. Such hyperpycnal flows are thought to be common at the mouths of medium to large rivers associated with low-gradient terrestrial catchments, and to be able to cover distances of up to several hundred kilometers (Zavala, 2020).

4.1.2.2 Seafloor Depth at the Canyon Apex

Inverse relationships of average canyon width (**Figure 7A**) and maximum (**Figure 7B**) and average canyon depth (**Figure 7C**) with seafloor depth at the canyon apex seen for canyons from passive margins might reflect how canyons with apices located at greater water depths are more likely to be disconnected from terrestrial and intrashelf sources, at present and during past sea-level lowstands. Unless such canyons are coupled with a

contouritic system (e.g., Warratz et al., 2019), intra-canyon erosion would be limited to mass-wasting events on the slope proximal to and within the canyon, and to wave erosion.

Active-margin canyons tend to have steeper sidewalls if their canyon apex is closer to the shoreline (Figure 7G) and/or at shallower seafloor depth (Figure 7E), whereas in passive margins the maximum canyon sidewall steepness does not correlate with either physiographic parameter (Figures 7E,G). This finding supports our hypothesis that erosive flows originating from within the shelf and terrestrial catchment may be more important in carving steep canyon walls in active settings compared to passive ones (Section 4.1.1). We also find that average canyon sinuosity and $w_{d_{max}}$ ratios of canyons in active settings show moderate scaling with canyon bathymetry at the apex, inverse for the former (Figure 7D) and positive for the latter (Figure 7F), which can also be ascribed to the influence of such erosive flows.

4.1.3 Sediment Supply to Shelf Margins

The moderate scaling of shelf-break depth with canyon length (Figure 8M), maximum width (Figure 8N) and depth (Figure 8O), and average canyon sinuosity (Figure 8P) for passive-margin canyons might reflect to some degree how higher rates of sediment supply from terrestrial source areas promote subsidence along continental margins and act to push the slope break into deeper waters (cf. Sweet and Blum, 2016; Wang et al., 2019). In contrast, relationships between the shelf-break depth and maximum canyon dimensions and overall canyon sinuosity are weak for active-margin canyons (Figures 8M–P), even though terrestrial catchments in active margins can be characterized by high rates of sediment supply (see also Section 4.1.2 and Section 4.1.4), which can be associated with narrow shelves promoting sediment routing to canyons (e.g., Blum and Hattier-Womack, 2009). Our observation may reflect, in part, the relative importance of structural controls on geomorphologic evolution in active settings (see Section 4.1.4), including the structural control of shelf-break migration (e.g., Han et al., 2016).

4.1.4 Structural Controls

Faulting and diapirism and their effects related to both gravitational failure and tectonic activity (e.g., Rowan et al., 2004; Hudec and Jackson, 2007; Yang et al., 2020) constitute structural controls that might affect canyon geomorphology in different ways through their influence on sediment-transport and canyon pathways (e.g., Chiang et al., 2012; Doo et al., 2015; Urías Espinosa et al., 2016); they can also do so by reshaping canyon walls (e.g., Yu and Chang, 2002; Bernhardt et al., 2015).

The greater impact of faulting and diapirism linked to tectonic activity on margin configuration, seafloor topography and sedimentary processes in active-margin settings compared to passive-margin ones (e.g., Yang et al., 2020) may explain some of the differences in scaling and canyon-morphometric characteristics seen between canyons across different tectonic settings.

The value of slope width for predicting canyon length (Sømme et al., 2009; Bührig et al., in review) is lower in active margins than

in passive ones (Figure 8R), which is possibly related to a greater and more prolonged impact of tectonic convergence on slope physiography in active margins compared to passive margins (e.g., Pratson et al., 2007; Yang et al., 2020), and its variable influence on canyon length. Canyon pathways can be deflected by positive topography created by faults and diapirs (e.g., Li et al., 2021), or develop along intraslope depressions as transform faults (e.g., Greene et al., 1991), or axes of intraslope basins (e.g., Bourget et al., 2010), thereby increasing canyon length relative to the width of the slope. On the other hand, emerging seafloor topography can lead to canyon abandonment by redirecting sediment pathways (e.g., Chiang et al., 2012), whereas the presence of intraslope basins (e.g., Harris et al., 2014a) and highs (e.g., Hsiung et al., 2014) can inhibit further extension of the canyon across the slope.

Given the general importance of structural controls on canyon length and average canyon sinuosity in active margins, it is unsurprising that our results indicate that both canyon morphometric parameters are not generally different between the different categories of active margins (convergent, transform and complex settings; Figures 4A,D).

In contrast, the fact that the maximum width of canyons from complex settings is on average larger compared to that of canyons from convergent and transform ones (Figure 4B) suggests that such settings may be inherently more favorable to the development of wide canyons. In tectonically complex settings with strike-slip tectonics, such as the Cook Strait sector, New Zealand, and offshore Taiwan in the East China Sea, a local widening of canyons might be promoted by the concurrence of transform faulting coupled with recurrent sediment gravity flows, where canyons intersect with strike-slip faults (e.g., Schnürle et al., 1998; Micallef et al., 2014).

In case of the SW Taiwan margin canyons, instead, the development of very wide canyons might be explained by the high frequency of hyperpycnal flows at river mouths (e.g., Milliman and Kao, 2005; Liu et al., 2013). The formation of hyperpycnal flows in the region is favored by enhanced erosion rates in terrestrial catchments from earthquake-related landslides (e.g., Dadson et al., 2005), extended periods of precipitation during the monsoonal wet season (e.g., Zhang et al., 2022) and associated with typhoons (e.g., Dadson et al., 2005; Milliman and Kao, 2005; Zhang et al., 2018), as well as from decreased levels of salinity of the ambient oceanic water due to high freshwater discharge along the margin (e.g., Dadson et al., 2005).

Despite the fact that both mean canyon length (Figure 2A) and mean maximum canyon depth (Figure 2D) are not significantly different in active and passive margins, length-to-maximum depth (ld_{max}) ratios are on average significantly higher in active margins (Figure 3C). The findings might reflect how enhanced seafloor relief linked to tectonics tends to increase canyon length, while simultaneously inhibiting canyon deepening. A downcanyon decrease in the erosive power of canyon-traversing flows may be caused by the capture of coarser sediment fractions by intraslope depressions (e.g., Soutter et al., 2021) and by flow deceleration upstream of slope topography leading to deposition of coarser sediment (e.g., Soutter et al., 2020). Although our data on the average

depth of canyons from active and passive margins show that active-margin canyons tend to be significantly shallower (**Figure 2E**), further investigation is needed to corroborate our findings in view of the limited geographic coverage of the dataset.

4.2 Canyon Geomorphology and Associated Characters of Deep-Water Systems

Despite the importance of sediment connection of submarine canyons to sediment sources in terrestrial catchments, shelves and slopes, and the lithological characteristics of source areas for the evolution of deep-water systems (e.g., Normark and Carlson, 2003; Smith et al., 2017; Hessler and Fildani, 2019; Bernhardt and Schwanghart, 2021), the character of a deep-water system is ultimately controlled by the efficiency of sediment transport through canyons to deep-marine sinks (Hessler and Fildani, 2019).

Stratigraphic forward modelling experiments by Wan et al. (2021) for delta-canyon-fan systems in a passive-margin setting suggest that sediment routing to basin floor sinks is promoted for shallow and low-sinuosity canyons.

Results by Wan et al. (2021) suggest that intracanyon basinward transport of coarser grain-size fractions is more efficient in shallower canyons. Canyons along active margins tend to be shallower than passive-margin canyons (**Figure 2E**), but they also tend to exhibit increased intra-canyon relief, which can inhibit the down-canyon erosive strength of flows *via* mass extraction (see **Section 4.1.4**). This suggests that the relationship identified by Wan et al. (2021) might not be applicable for canyons in active-margin settings. Similarly, the impact of canyon depth on grain-size segregation within canyons might be subdued in canyons associated with passive-margin settings where slope relief is increased by gravitational loading.

The rate of thalweg lateral migration, which determines the canyon sinuosity, controls the caliber of sediment transported down-canyon; in more sinuous canyons, a relatively larger proportion of coarse sediment is deposited along the inner bends and the proximal part of the canyon, whereas in canyons with lower sinuosity the coarser sediment can be more effectively transported down-slope (Wan et al., 2021). Given that the average sinuosity of canyons is neither generally different between active and passive margins (**Figure 2F** this study; Harris and Whiteway, 2011; Bührig et al., in review), nor seemingly different across the considered active-margin settings (**Figure 4D**), the control of canyon sinuosity on sediment transport dynamics and grain-size segregation is probably not fundamentally different between active- and passive-margin settings and across active margins with different types of plate boundaries.

However, the influence of canyon geomorphology on sediment connection across deep-water environments might be absent or less prominent for active margins where canyons experience “flushing” initiated by large-magnitude earthquakes (e.g., Goldfinger et al., 2012; Atwater et al., 2014), due to the remobilization of large volumes of sediment, including coarser grain size fractions, and related substrate erosion within the canyon (e.g., Mountjoy et al., 2018).

These aspects highlight the need for modelling studies and conceptual models of S2S and deep-water systems to better consider the wide range of boundary conditions associated with characteristics of continental margins.

4.3 Implications of the Findings and Future Work

Our comparisons of frequency distributions of canyon morphometric parameters for different tectonic settings (**Figures 2A–H, 4A–I**) corroborate results of earlier quantitative global studies, showing that canyon morphometrics are variably sensitive to factors related to the tectonic-margin type (e.g., Harris and Whiteway, 2011; Bührig et al., in review). These insights suggest that overall canyon geomorphology cannot be predicted from the tectonic setting alone. Our findings that canyons along active margins display a greater variability in aspect ratios of maximum canyon dimensions (**Figures 3A–C**) indicate that the size of canyon fills in the stratigraphic record might be less reliably estimated from outcrop and subsurface data in active-margin settings compared to passive margins. Moreover, aspects of canyon morphometry in canyons associated with convergent settings are not fundamentally different compared to those in complex settings (**Figures 4A–I**), suggesting that canyon geomorphology is not primarily controlled by the complexity of the tectonic regime in active-margin settings. Despite this, complex tectonics may be preferentially associated with canyons with larger maximum widths and depths (**Figures 4B,C**, see also **Section 4.1.4**).

Our analysis also shows that scaling relationships of canyon morphometric parameters with attributes of the physiographic setting (**Figures 6A,B, 7A–H**) and source-to-sink (S2S) system (**Figures 8A–R, 9A,B**) might vary between active and passive margins. The same applies for scaling relationships between the different canyon morphometric parameters (**Figures 5A–G**), and for scaling between attributes of S2S systems (**Figures 11A,B**). These findings are important because they demonstrate that the relationships between continental-margin types and the configuration of deep-water systems is more complex than hitherto recognized in conceptual, experimental and numerical models.

The variable and complex influence of the tectonic setting on sediment routing along S2S systems, on canyon geomorphology, and on the degree of confinement of deep-water fans in settings such as intraslope basins (e.g., Budillon et al., 2011; Hsiung et al., 2014), lower slopes with complex seafloor topography (e.g., Hsiung et al., 2018), and trenches (e.g., Thornburg et al., 1990; McArthur and Tek, 2021) raises the question whether scaling relationships between submarine canyons and deep-water fans can be predicted. This needs to be investigated in future work.

5 CONCLUSION

A global metastudy of geomorphic characteristics of submarine canyons as a function of the tectonic setting has been conducted. The key findings of the study are that:

- 1) Overall canyon geomorphology is not generally different between active and passive margins and across different plate-boundary types in tectonically active settings.
- 2) The role of slope failure as a mechanism governing the morphology of canyons may be subordinate for canyons associated with active margins, compared to passive-margin examples, possibly due to seismic strengthening of seafloors in the former. This indicates that width-to-depth ratios might be inherently limited in their magnitude in canyons in passive-margin settings due to the interplay of intracanyon sediment flows and canyon-wall failure, with the latter counteracting canyon-margin accretion while promoting canyon widening and aggradation of canyon floors.
- 3) Scaling relationships of individual canyon morphometric parameters and aspect ratios of maximum canyon dimensions with attributes of the S2S system and the physiographic setting have been demonstrated for 1) active margins, 2) passive margins, and 3) across both margin types. The scaling relationships vary broadly in magnitude of correlation, but are seldom strong; this reflects how canyon geomorphology is shaped by the complex interplay of different controls, which are only in part influenced by the tectonic setting.
- 4) Our findings suggest that canyon geomorphology can be to some degree predicted in S2S systems in active and passive margins, but that the predictive value of attributes of the environmental setting might vary across different tectonic settings.
- 5) Insights from this study suggest possible genetic links between aspects of canyon geomorphology and characteristics of the physiographic environment related to the tectonic setting. This finding can be applied to improve and help constrain conceptual, experimental and numerical models of submarine canyons and canyon-associated sedimentary systems at source-to-sink scale by 1) demonstrating how the relative importance of controlling factors on canyon morphometry might vary across different tectonic settings; 2) providing a quantitative characterization of canyon morphometric attributes and associated parameters of the physiographic and environmental setting that can be applied to constrain models in a realistic manner; and 3) illustrating how insights from our analyses can augment existing semi-quantitative models of source-to-sink systems for different tectonic settings, which have not yet expressly considered submarine-canyon morphometry (e.g., Sømme et al., 2009; Nyberg et al., 2018).

REFERENCES

- Acosta, J., Canals, M., López-MartínezMuñoz, A., Herranz, P., Urgeles, R., et al. (2002). The Balearic Promontory Geomorphology (Western Mediterranean): Morphostructure and Active Processes. *Geomorphology* 49, 177–204.
- Alford, M. H., and MacCready, P. (2014). Flow and Mixing in Juan de Fuca Canyon, Washington. *Geophys. Res. Lett.* 41, 1608–1615. doi:10.1002/2013GL058967
- Allen, S. E., Vindeirinho, C., Thomson, R. E., Foreman, M. G., and Mackas, D. L. (2001). Physical and Biological Processes Over a Submarine Canyon During an Upwelling Event. *Can. J. Fish. Aquat. Sci.* 58, 671–684. doi:10.1139/cjfas-58-4-67110.1139/f01-008

DATA AVAILABILITY STATEMENT

The raw data supporting the conclusion of this article will be made available by the authors, without undue reservation.

AUTHOR CONTRIBUTIONS

LB conceptualized and led the investigation, conducted the analyses, drafted the figures and wrote the original draft. LC, MP, NM, and WM supervised the project. LC, MP, NM, and WM provided specialist technical input for the interpretation of geomorphological and geological datasets and the application of statistical analytical techniques; they additionally contributed to the scientific writing of the manuscript and to manuscript revisions.

FUNDING

This research was funded by the sponsors of the Turbidites Research Group (AkerBP, CNOOC, ConocoPhillips, Harbour, Murphy, Occidental, OMV) and of the Fluvial, Eolian & Shallow-Marine Research Group [AkerBP, Areva (now Orano), BHP, Cairn India (Vedanta), Chevron, CNOOC International, ConocoPhillips, Equinor, Murphy Oil, Occidental, Petrotechnical Data Systems, Saudi Aramco, Shell, Tullow Oil, Woodside, YPF], School of Earth and Environment, University of Leeds. Financial support to this research was also provided by NERC (NE/P01691X/1).

ACKNOWLEDGMENTS

We thank the sponsors of the Turbidites Research Group and of the Fluvial, Eolian & Shallow-Marine Research Group for financial support. We thank DC and AF for their constructive comments, which helped improve the paper.

SUPPLEMENTARY MATERIAL

The Supplementary Material for this article can be found online at: <https://www.frontiersin.org/articles/10.3389/feart.2022.836823/full#supplementary-material>

- Allin, J. R., Hunt, J. E., Talling, P. J., Clare, M. A., Pope, E., and Masson, D. G. (2016). Different Frequencies and Triggers of Canyon Filling and Flushing Events in Nazaré Canyon, Offshore Portugal. *Mar. Geol.* 371, 89–105. doi:10.1016/j.margeo.2015.11.005
- Almagor, G. (1993). Continental Slope Processes off Northern Israel and Southernmost Lebanon and Their Relation to Onshore Tectonics. *Mar. Geol.* 112, 151–169. doi:10.1016/0025-3227(93)90166-s
- Alonso, B., and Ercilla, G. (2003). Small Turbidite Systems in a Complex Tectonic Setting (SW Mediterranean Sea): Morphology and Growth Patterns. *Mar. Pet. Geol.* 19, 1225–1240. doi:10.1016/S0264-8172(03)00036-9
- Amblas, D., Ceramicola, S., Gerber, T. P., Canals, M., Chiocci, F. L., Dowdeswell, J. A., et al. (2017). “Submarine Canyons and Gullies,” in *Submarine*

- Geomorphology*. Editors A. Micallef, S. Krastel, and A. Savini (Berlin, Germany: Springer), 251–272. doi:10.1007/978-3-319-57852-1_14
- Amblas, D., Gerber, T. P., De Mol, B., Urgeles, R., Garcia-Castellanos, D., Canals, M., et al. (2012). Survival of a Submarine Canyon during Long-Term Outbuilding of a Continental Margin. *Geology* 40 (6), 543–546. doi:10.1130/G33178.1
- Antobreh, A. A., and Krastel, S. (2006). Morphology, Seismic Characteristics and Development of Cap Timiris Canyon, Offshore Mauritania: a Newly Discovered Canyon Preserved-Off a Major Arid Climatic Region. *Mar. Petroleum Geol.* 23, 37–59. doi:10.1016/j.marpetgeo.2005.06.003
- Armitage, D. A., Piper, D. J. W., McGee, D. T., and Morris, W. R. (2010). Turbidite Deposition on the Glacially Influenced, Canyon-Dominated Southwest Grand Banks Slope, Canada. *Sedimentology* 57, 1387–1408. doi:10.1111/j.1365-3091.2010.01149.x
- Arzola, R. G., Wynn, R. B., Lastras, G., Masson, D. G., and Weaver, P. P. E. (2008). Sedimentary Features and Processes in the Nazaré and Setúbal Submarine Canyons, West Iberian Margin. *Mar. Geol.* 250, 64–88. doi:10.1016/j.margeo.2007.12.006
- Atwater, B. F., Carson, B., Griggs, G. B., Johnson, H. P., and Salmi, M. S. (2014). Rethinking Turbidite Paleoseismology Along the Cascadia Subduction Zone. *Geology* 42, 827–830. doi:10.1130/G35902.1
- Babonneau, N., Delacourt, C., Cancouët, R., Sisavath, E., Bachèlery, P., Mazuel, A., et al. (2013). Direct Sediment Transfer From Land to Deep-Sea: Insights into Shallow Multibeam Bathymetry at La Réunion Island. *Mar. Geol.* 346, 47–57. doi:10.1016/j.margeo.2013.08.006
- Babonneau, N., Savoye, B., Cremer, M., and Klein, B. (2002). Morphology and Architecture of the Present Canyon and Channel System of the Zaire Deep-Sea Fan. *Mar. Petroleum Geol.* 19, 445–467. doi:10.1016/s0264-8172(02)00009-0
- Baker, E. T., and Hickey, B. M. (1986). Contemporary Sedimentation Processes in and Around an Active West Coast Submarine Canyon. *Mar. Geol.* 71, 15–34. doi:10.1016/0025-3227(86)90031-9
- Baztan, J., Berné, S., Olivet, J.-L., Rabineau, M., Aslanian, D., Gaudin, M., et al. (2005). Axial Incision: The Key to Understand Submarine Canyon Evolution (In the Western Gulf of Lion). *Mar. Pet. Geol.* 22 (6–7), 805–826. doi:10.1016/j.marpetgeo.2005.03.011
- Bernhardt, A., Melnick, D., Jara-Muñoz, J., Argandoña, B., González, J., and Strecker, M. R. (2015). Controls on Submarine Canyon Activity during Sea-Level Highstands. The Biobío Canyon System Offshore Chile. *Geosphere* 11 (4), 1226–1255. doi:10.1130/GES01063.1
- Bernhardt, A., and Schwanghart, W. (2021). Where and Why Do Submarine Canyons Remain Connected to the Shore during Sea-Level Rise? Insights from Global Topographic Analysis and Bayesian Regression. *Geophys. Res. Lett.* 48, e2020GL092234. doi:10.1029/2020GL092234
- Blum, M. D., and Hattier-Womack, J. (2009). “Climate Change, Sea-Level Change, and Fluvial Sediment Supply to Deepwater Depositional Systems,” in *External Controls on Deep Water Depositional Systems: Climate, Sea-Level, and Sediment Flux*. Editors B. Kneller, O. J. Martinsen, and B. McCaffrey (Tulsa, OK: SEPM), 15–40. doi:10.2110/sepmsp.092.015
- Bosley, K. L., Lavelle, J. W., Brodeur, R. D., Wakefield, W. W., Emmet, R. L., Baker, E. T., et al. (2004). Biological and Physical Processes in and Around Astoria Submarine Canyon, Oregon, USA. *J. Mar. Syst.* 50, 21–37. doi:10.1016/j.jmarsys.2003.06.006
- Bouma, A. H., and Scott, E. D. (2003). “Source-to-sink: the Importance of the Updip Coastal Area in Defining Deep-Water Sand Characteristics,” in *Shelf Margin Deltas and Linked Down Slope Petroleum Systems – Global Significance and Future Exploration Potential*. Editors H. H. Roberts, N. C. Rosen, R. H. Fillon, and J. B. Anderson (Houston, TX: GCSSEPM), 597–617. doi:10.5724/gcs.03.23.0597
- Bourget, J., Zaragosi, S., Ellouz-Zimmermann, N., Mouchot, N., Garlan, T., Schneider, J.-L., et al. (2010). Turbidite System Architecture and Sedimentary Processes along Topographically Complex Slopes: the Makran Convergent Margin. *Sedimentology* 58 (2), 376–406. doi:10.1111/j.1365-3091.2010.01168.x
- Budillon, F., Conforti, A., Tonielli, R., De Falco, G., Di Martino, G., Innangi, S., et al. (2011). The Bulgheria Canyon-Fan: A Small-Scale Proximal System in the Eastern Tyrrhenian Sea (Italy). *Mar. Geophys. Res.* 32, 83–97. doi:10.1007/s11001-011-9138-9
- Bührig, L. H., Colomera, L., Patacci, M., Mountney, N. P., and McCaffrey, W. D. (in review). A Global Analysis of Controls on Submarine-Canyon Geomorphology. *arXiv*. doi:10.31223/X5RK9H
- Çağatay, M. N., Uçarkus, G., Eriş, K. K., Henry, P., Gasperini, L., and Polonia, A. (2015). “Submarine Canyons of the Sea of Marmara,” in *Submarine Canyon Dynamics in the Mediterranean and Tributary Seas – an Integrated Geological, Oceanographic and Biological Perspective*. Editor F. Briand (Monaco:CIESM), 123–135.
- Carlson, P. R., Bruns, T. R., and Fisher, M. A. (1990). “Development of Slope Valleys in the Glacimarine Environment of a Complex Subduction Zone, Northern Gulf of Alaska,” in *Glacimarine Environments; Processes and Sediments*. Editors J. A. Dowdeswell and J. D. Scourse (London: GEOLOGICAL SOCIETY), 139–153. doi:10.1144/gsl.sp.1990.053.01.08
- Carlson, P. R., and Karl, H. A. (1988). Development of Large Submarine Canyons in the Bering Sea, Indicated by Morphologic, Seismic, and Sedimentologic Characteristics. *Geol. Soc. Am. Bull.* 100, 1594–1615. doi:10.1130/0016-7606(1988)100<1594:dolsci>2.3.co;2
- Carlson, P. R., and Karl, H. A. (1984). Discovery of Two New Large Submarine Canyons in the Bering Sea. *Mar. Geol.* 56, 159–179. doi:10.1016/0025-3227(84)90011-2
- Carson, B., Baker, E. T., Hickey, B. M., Nittrouer, C. A., DeMaster, D. J., Thorbjarnarson, K. W., et al. (1986). Modern Sediment Dispersal and Accumulation in Quinault Submarine Canyon – A Summary. *Mar. Geol.* 71, 1–13. doi:10.1016/0025-3227(86)90030-7
- Casalbore, D., Chiocci, F. L., Scarascia Mugnozza, G., Tommasi, P., and Sposato, A. (2011). Flash-flood Hyperpycnal Flows Generating Shallow-Water Landslides at Fiumara Mouths in Western Messina Strait (Italy). *Mar. Geophys. Res.* 32, 257–271. doi:10.1007/s11001-011-9128-y
- Casalbore, D., Falcini, F., Martorelli, E., Morelli, E., Bosman, A., Calarco, M., et al. (2018). Characterization of Overbanking Features on the Lower Reach of the Gioia-Mesima Canyon-Channel System (Southern Tyrrhenian Sea) through Integration of Morpho-Stratigraphic Data and Physical Modelling. *Prog. Oceanogr.* 169, 66–78. doi:10.1016/j.pcean.2018.02.020
- Chen, H., Zhan, W., Li, L., and Wen, M.-M. (2017). Occurrence of Submarine Canyons, Sediment Waves and Mass Movements along the Northern Continental Slope of the South China Sea. *J. Earth Syst. Sci.* 126, 73. doi:10.1007/s12040-017-0844-9
- Chiang, C.-S., and Yu, H.-S. (2006). Morphotectonics and Incision of the Kaoping Submarine Canyon, SW Taiwan Orogenic Wedge. *Geomorphology* 80, 199–213. doi:10.1016/j.geomorph.2006.02.008
- Chiang, C.-S., Yu, H.-S., Noda, A., TuZino, T., and Su, C.-C. (2012). Avulsion of the Fangleiao Submarine Canyon off Southwestern Taiwan as Revealed by Morphological Analysis and Numerical Simulation. *Geomorphology* 177–178, 26–37. doi:10.1016/j.geomorph.2012.07.011
- Coleman, J. M., Prior, D. B., and Lindsay, J. F. (1982). Formation of the Mississippi Canyon. *GCAGS Trans.* 32, 519.
- Corradino, M., Pepe, F., Burrato, P., Kanari, M., Parrino, N., Bertotti, G., et al. (2021). An Integrated Multiscale Method for the Characterization of Active Faults in Offshore Areas. The Case of Sant’Eufemia Gulf (Offshore Calabria, Italy). *Front. Earth Sci.* 9, 670557. doi:10.3389/feart.2021.670557
- Covault, J. A., Fildani, A., Romans, B. W., and McHargue, T. (2011a). The Natural Range of Submarine Canyon-And-Channel Longitudinal Profiles. *Geosphere* 7 (2), 313–332. doi:10.1130/GES00610.1
- Covault, J. A., Romans, B. W., Graham, S. A., Fildani, A., and Hilley, G. E. (2011b). Terrestrial Source to Deep-Sea Sink Sediment Budgets at High and Low Sea Levels: Insights from Tectonically Active Southern California. *Geology* 39 (7), 619–622. doi:10.1130/G31801.1
- Cullis, S., Patacci, M., Colomera, L., Bührig, L., and McCaffrey, W. D. (2019). A Database Solution for the Quantitative Characterisation and Comparison of Deep-Marine Siliciclastic Depositional Systems. *Mar. Pet. Geol.* 102, 321–339. doi:10.1016/j.marpetgeo.2018.12.023
- Dadson, S., Hovius, N., Pegg, S., Dade, W. B., Horng, M. J., and Chen, H. (2005). Hyperpycnal River Flows from an Active Mountain Belt. *J. Geophys. Res.* 110, F04016. doi:10.1029/2004JF000244
- Davies, H. L., Keene, J. B., Hashimoto, K., Joshima, M., Stuart, J. E., and Tiffin, D. L. (1987). Bathymetry and Canyons of the Western Solomon Sea. *Geo-Mar. Lett.* 6, 181–191.

- de Almeida, N. M., Vital, H., and Gomes, M. P. (2015). Morphology of Submarine Canyons along the Continental Margin of the Potiguar Basin, NE Brazil. *Mar. Pet. Geol.* 68, 307–324. doi:10.1016/j.marpetgeo.2015.08.035
- Dietz, R. S., Knebel, H. J., and Somers, L. H. (1968). Cayar Submarine Canyon. *Geol. Soc. Am. Bull.* 79, 1821–1828. doi:10.1130/0016-7606(1968)79[1821:nadcsj]2.0.co;2
- Ding, W., Li, J., Li, J., Fang, Y., and Tang, Y. (2013). Morphotectonics and Evolutionary Controls on the Pearl River Canyon System, South China Sea. *Mar. Geophys. Res.* 34, 221–238. doi:10.1007/s11001-013-9173-9
- Doo, W.-B., Hsu, S.-K., Lo, C.-L., Chen, S.-C., Tsai, C.-H., Lin, J.-Y., et al. (2015). Gravity Anomalies of the Active Mud Diapirs off Southwest Taiwan. *Geophys. J. Int.* 203, 2089–2098. doi:10.1093/gji/ggv430
- Eittrheim, S., Grantz, A., and Greenberg, J. (1982). Active Geologic Processes in Barrow Canyon, Northeast Chukchi Sea. *Mar. Geol.* 50, 61–76. doi:10.1016/0025-3227(82)90061-5
- Ercilla, G., Alonso, B., Perez-Belzuz, F., Estrada, F., Baraza, J., Farran, M., et al. (1998). Origin, Sedimentary Processes and Depositional Evolution of the Agadir Turbidite System, Central Eastern Atlantic. *J. Geol. Soc. Lond.* 155 (6), 929–939. doi:10.1144/gsjgs.155.6.0929
- Exon, N. F., Hill, P. J., Mitchell, C., and Post, A. (2005). Nature and Origin of the Submarine Albany Canyons off Southwest Australia. *Aust. J. Earth Sci.* 52 (1), 101–115. doi:10.1080/08120090500100036
- Ferry, J.-N., Babonneau, N., Mulder, T., Parize, O., and Raillard, S. (2004). Morphogenesis of Congo Submarine Canyon and Valley: Implications about the Theories of the Canyons Formation. *Geodin. Acta.* 17, 241–251. doi:10.3166/ga.17.241-251
- Fildani, A. (2017). Submarine Canyons: A Brief Review Looking Forward. *Geology* 45 (4), 383–384. doi:10.1130/focus042017.1
- Galewsky, J., and Silver, E. A. (1997). Tectonic Controls on Facies Transitions in an Oblique Collision: The Western Solomon Sea, Papua New Guinea. *Am. Geol. Soc. Bull.* 109 (10), 1266–1278. doi:10.1130/0016-7606(1997)109<1266:tcft>2.3.co;2
- Gamberi, F., Rovere, M., Marani, M. P., and Dykstra, M. (2015). Modern Submarine Canyon Feeder-System and Deep-Sea Fan Growth in a Tectonically Active Margin (Northern Sicily). *Geosphere* 11 (2), 307–319. doi:10.1130/GES01030.1
- Gardner, J. V., Dartnell, P., Mayer, L. A., and Hughes Clarke, J. E. (2003). Geomorphology, Acoustic Backscatter, and Processes in Santa Monica Bay from Multibeam Mapping. *Mar. Environ. Res.* 56, 15–46. doi:10.1016/S0141-1136(02)00323-9
- Gardner, W. D., Glover, L. K., and Hollister, C. D. (1980). Canyons off Northwest Puerto Rico: Studies of Their Origin and Maintenance with the Nuclear Research Submarine NR-1. *Mar. Geol.* 37, 41–70. doi:10.1016/0025-3227(80)90011-0
- Gervais, A., Mulder, T., Savoye, B., and Gonthier, E. (2006). Sediment Distribution and Evolution of Sedimentary Processes in a Small Sandy Turbidite System (Golo System, Mediterranean Sea): Implications for Various Geometries Based on Core Framework. *Geo-Mar. Lett.* 26, 373–395. doi:10.1007/s00367-006-0045-z
- Gervais, A., Savoye, B., Piper, D. J. W., Mulder, T., Cremer, M., and Pichevin, L. (2004). “Present Morphology and Depositional Architecture of a Sandy Confined Submarine System: the Golo Turbidite System (Eastern Margin of Corsica),” in *Confined Turbidite Systems*. Editors S. A. Lomas and P. Joseph (London: Geological Society), 59–89. doi:10.1144/gsl.sp.2004.222.01.05
- Gnibidenko, H. S., and Svarichevskaya, L. V. (1984). The Submarine Canyons of Kamchatka. *Mar. Geol.* 54, 277–307. doi:10.1016/0025-3227(84)90043-4
- Goldfinger, C., Nelson, C. H., Morey, A. E., Johnson, J. R., Patton, J., Karabanov, E., et al. (2012). Turbidite Event History – Methods and Implications for Holocene Paleoseismicity of the Cascadia Subduction Zone. *USGS Prof. Pap.* 1661-F, 170. doi:10.3133/PP1661F
- Gómez-Ballesteros, M., Druet, M., Muñoz, A., Arrese, B., Rivera, J., Sánchez, F., et al. (2014). Geomorphology of the Avilés Canyon System, Cantabrian Sea (Bay of Biscay). *Deep Sea Res. Part II Top. Stud. Oceanogr.* 106, 99–117. doi:10.1016/j.dsr2.2013.09.031
- Greene, H. G., Clarke, S. H., Jr., and Kennedy, M. P. (1991). “Tectonic Evolution of Submarine Canyons along the California Continental Margin,” in *From Shoreline to Abyss: Contributions in Marine Geology in Honor of Francis Parker Shepard*. Editor R. H. Osborne (Tulsa, OK: SEPM), 231–248. doi:10.2110/pec.91.09.0231
- Greene, H. G., Maher, N. M., and Paull, C. K. (2002). Physiography of the Monterey Bay National Marine Sanctuary and Implications about Continental Margin Development. *Mar. Geol.* 181, 55–82. doi:10.1016/S0025-3227(01)00261-4
- Hagen, R. A., Bergersen, D. D., Moberly, R., and Coulbourn, W. T. (1994). Morphology of a Large Meandering Submarine Canyon System on the Peru-Chile Forearc. *Mar. Geol.* 119, 7–38. doi:10.1016/0025-3227(94)90138-4
- Hagen, R. A., Vergara, H., and Naar, D. F. (1996). Morphology of San Antonio Submarine Canyon on the Central Chile Forearc. *Mar. Geol.* 129, 197–205. doi:10.1016/0025-3227(96)83345-7
- Han, J., Xu, G., Li, Y., and Zhuo, H. (2016). Evolutionary History and Controlling Factors of the Shelf Breaks in the Pearl River Mouth Basin, Northern South China Sea. *Mar. Pet. Geol.* 77, 179–189. doi:10.1016/j.marpetgeo.2016.06.009
- Han, X., Li, J., Chu, F., Li, J., and Yang, F. (2010). “Geomorphology and Tectonic Interpretation of Zhujiang Submarine Canyon, in the Northern South China Sea,” in OCEANS’10 IEEE SYDNEY, Sydney, NSW, Australia, May 24–27, 2010. doi:10.1109/OCEANSSYD.2010.5603638
- Harris, P. T., Barrie, J. V., Conway, K. W., and Greene, H. G. (2014a). Hanging Canyons of Haida Gwaii, British Columbia, Canada: Fault-Control on Submarine Canyon Geomorphology along Active Continental Margins. *Deep Sea Res. Part II Top. Stud. Oceanogr.* 104, 83–92. doi:10.1016/j.dsr2.2013.06.017
- Harris, P. T., Macmillan-Lawler, M., Rupp, J., and Baker, E. K. (2014b). Geomorphology of the Oceans. *Mar. Geol.* 352, 4–24. doi:10.1016/j.margeo.2014.01.011
- Harris, P., and Whiteway, T. (2011). Global Distribution of Large Submarine Canyons: Geomorphic Differences between Active and Passive Continental Margins. *Mar. Geol.* 285, 69–86. doi:10.1016/j.margeo.2011.05.008
- Hessler, A. M., and Fildani, A. (2019). Deep-sea Fans: Tapping into Earth’s Changing Landscapes. *J. Sediment. Res.* 89 (11), 1171–1179. doi:10.2110/jsr.2019.64
- Hickey, B. M. (1997). The Response of a Steep-Sided, Narrow Canyon to Time-Varying Wind Forcing. *J. Phys. Oceanogr.* 27 (5), 697–726. doi:10.1175/1520-0485(1997)027<0697:troass>2.0.co;2
- Hodgson, D. M., Kane, I. A., Flint, S. S., Brunt, R. L., and Ortiz-Karppf, A. (2016). Time-transgressive Confinement on the Slope and the Progradation of Basin-Floor Fans: Implications for the Sequence Stratigraphy of Deep-Water Deposits. *J. Sediment. Res.* 86, 73–86. doi:10.2110/jsr.2016.3
- Hsiung, K.-H., Kanamatsu, T., Ikehara, K., Shiraiishi, K., Horng, C.-S., and Usami, K. (2017). Morpho-sedimentary Features and Sediment Dispersal Systems of the Southwest End of the Ryukyu Trench: a Source-To-Sink Approach. *Geo-Mar. Lett.* 37, 561–577. doi:10.1007/s00367-017-0509-3
- Hsiung, K.-H., Yu, H.-S., and Chiang, C.-S. (2014). Seismic Characteristics, Morphology and Formation of the Ponged Fangliao Fan off Southwestern Taiwan, Northern South China Sea. *Geo-Mar. Lett.* 34, 59–74. doi:10.1007/s00367-013-0351-1
- Hsiung, K.-H., Yu, H.-S., and Chiang, C.-S. (2018). The Modern Kaoping Transient Fan Offshore SW Taiwan: Morphotectonics and Development. *Geomorphology* 300, 151–163. doi:10.1016/j.geomorph.2017.10.013
- Hsiung, K.-H., and Yu, H.-S. (2011). Morpho-Sedimentary Evidence for a Canyon-Channel-Trench Interconnection Along the Taiwan-Luzon Plate Margin, South China Sea. *Geo-Mar. Lett.* 31, 215–226. doi:10.1007/s00367-010-0226-7
- Hsu, S.-K., Kuo, J., Lo, C.-L., Tsai, C.-H., Doo, W.-B., Ku, C.-Y., et al. (2008). Turbidity Currents, Submarine Landslides and the 2006 Pingtung Earthquake off SW Taiwan. *Terr. Atmos. Ocean. Sci.* 19 (6), 767–772. doi:10.3319/tao.2008.19.6.767(pt)
- Huang, z., Nichol, S. L., Harris, P. T., and Caley, M. J. (2014). Classification of Submarine Canyons of the Australian Continental Margin. *Mar. Geol.* 357, 362–383. doi:10.1016/j.margeo.2014.07.007
- Hudec, M. R., and Jackson, M. P. A. (2007). Terra Infirmis: Understanding Salt Tectonics. *Earth-Sci. Rev.* 82, 1–28. doi:10.1016/j.earscirev.2007.01.001
- Ingersoll, R. V. (2012). “Chapter 1: Tectonics of Sedimentary Basins, with Revised Nomenclature,” in *Tectonics of Sedimentary Basins: Recent Advances*. Editors C. Busby and A. Azor (Oxford, UK: Blackwell Publishing), 3–43.
- Jimoh, R. O., Tang, Y., Li, J., Awosika, L. F., Li, H., Akinnibage, E. A., et al. (2018). The Architecture of the Lower Parts of Submarine Canyons on the Western

- Nigerian Continental Margin. *Acta Oceanol. Sin.* 37 (7), 28–40. doi:10.1007/s13131-018-1242-0
- Ju, Y., Wang, G., Li, S., Sun, Y., Suo, Y., Somerville, I., et al. (2020). Geodynamic Mechanism and Classification of Basins in the Earth System. *Gondwana Res.* 2020. In press. doi:10.1016/j.gr.2020.08.017
- Khripounoff, A., Crassous, P., Bue, N. L., Dennielou, B., and Jacinto, R. S. (2012). Different Types of Sediment Gravity Flows Detected in the Var Submarine Canyon (Northwestern Mediterranean Sea). *Progr. Oceanogr.* 106, 138–153. doi:10.1016/j.pocean.2012.09.001
- Klaus, A., and Taylor, B. (1991). Submarine Canyon Development in the Izu-Bonin Forearc: a SeaMARC II and Seismic Survey of Aoga Shima Canyon. *Mar. Geophys. Res.* 13, 131–152.
- Krastel, S., Hanebuth, T. J. J., Antobreh, A. A., Henrich, R., Holz, C., Kölling, M., et al. (2004). Cap Timiris Canyon: a Newly Discovered Channel System Offshore of Mauritania. *Eos Trans. Am. Geophys. Union.* 85 (42), 417–432. doi:10.1029/2004eo420001
- Krastel, S., Wefer, G., Hanebuth, T. J. J., Antobreh, A. A., Freudenthal, T., Preu, B., et al. (2011). M78/3 shipboard scientific party Sediment dynamics and geohazards off Uruguay and the de la Plata River region (northern Argentina and Uruguay). *Geo-Mar. Lett.* 31, 271–283. doi:10.1007/s00367-011-0232-4
- Lastras, G., Acosta, J., Muñoz, A., and Canals, M. (2011a). Submarine Canyon Formation and Evolution in the Argentine Continental Margin Between 44°30'S and 48°S. *Geomorphology* 128, 116–136. doi:10.1016/j.geomorph.2010.12.027
- Lastras, G., Arzola, R. G., Masson, D. G., Wynn, R. B., Huvenne, V. A. I., Hühnerbach, V., et al. (2009). Geomorphology and Sedimentary Features in the Central Portuguese Submarine Canyons, Western Iberian Margin. *Geomorphology* 103, 310–329. doi:10.1016/j.geomorph.2008.06.013
- Lastras, G., Canals, M., Amblas, D., Lavoie, C., Church, I., De mol, B., et al. (2011b). Understanding Sediment Dynamics of Two Large Submarine Valleys from Seafloor Data: Blanes and La Fonera Canyons, Northwestern Mediterranean Sea. *Mar. Geol.* 280, 20–39. doi:10.1016/j.margeo.2010.11.005
- Lastras, G., Canals, M., Urgeles, R., Amblas, D., Ivanov, M., Droz, L., et al. (2007). A Walk Down the Cap de Creus Canyon, Northwestern Mediterranean Sea: Recent processes inferred from morphology and sediment bedforms. *Mar. Geol.* 246, 176–192. doi:10.1016/j.margeo.2007.09.002
- Laursen, J., and Normark, W. R. (20022002). Late Quaternary Evolution of the San Antonio Submarine Canyon in the Central Chile Forearc (~33°S). *Mar. Geol.* 188, 365–390. doi:10.1016/s0025-3227(02)00421-8
- Le Dantec, N., Hogarth, L. J., Driscoll, N. W., Babcock, J. M., Barnhardt, W. A., and Schwab, W. C. (2010). Tectonic Controls on Nearshore Sediment Accumulation and Submarine Canyon Morphology Offshore La Jolla, Southern California. *Mar. Geol.* 268, 115–128. doi:10.1016/j.margeo.2009.10.026
- Lewis, K. B., and Barnes, P. M. (1999). Kaikoura Canyon, New Zealand: Active Conduit from Near-Shore Sediment Zones to Trench-Axis Channel. *Mar. Geol.* 162, 39–69. doi:10.1016/s0025-3227(99)00075-4
- Li, M. Z., Prescott, R. H., and Robertson, A. G. (2019). Observation of Internal Tides and Sediment Transport Processes at the Head of Logan Canyon on Central Scotian Slope, Eastern Canada. *J. Mar. Syst.* 193, 103–125. doi:10.1016/j.jmarsys.2019.02.007
- Li, W., Li, S., Alves, T. M., Rebesco, M., and Feng, Y. (2021). The Role of Sediment Gravity Flows on the Morphological Development of a Large Submarine Canyon (Taiwan Canyon), North-East South China Sea. *Sedimentology* 68, 1091–1108. doi:10.1111/sed.12818
- Liu, J. T., Hsu, R. T., Hung, J.-J., Chang, Y.-P., Wang, Y.-H., Rendle-Bühning, R. H., et al. (2016). From the Highest to the Deepest: The Gaoping River-Gaoping Submarine Canyon Dispersal System Earth-. *Sci. Rev.* 153, 274–300. doi:10.1016/j.earscrev.2015.10.012
- Liu, J. T., Kao, S.-J., Huh, C.-A., and Hung, C.-C. (2013). Gravity Flows Associated with Flood Events and Carbon Burial: Taiwan as Instructional Source Area. *Annu. Rev. Mar. Sci.* 5, 47–68. doi:10.1146/annurev-marine-121211-172307
- Lo Iacono, C., Sulli, A., Agate, M., Lo Presti, V., Pepe, F., and Catalano, R. (2011). Submarine Canyon Morphologies in the Gulf of Palermo (Southern Tyrrhenian Sea) and Possible Implications for Geo-Hazard. *Mar. Geophys. Res.* 32, 127–138. doi:10.1007/s11001-011-9118-0
- Lo Iacono, C., Sulli, A., and Agate, M. (2014). Submarine Canyons of North-Western Sicily (Southern Tyrrhenian Sea): Variability in Morphology, Sedimentary Processes and Evolution on a Tectonically Active Margin. *Deep Sea Res. Part II Top. Stud. Oceanogr.* 104, 93–105. doi:10.1016/j.dsr2.2013.06.018
- Maier, K. L., Rosenberger, K. J., Paull, C. K., Gwiazda, R., Gales, J., Lorenson, T., et al. (2019). Sediment and Organic Carbon Transport and Deposition Driven by Internal Tides along Monterey Canyon, Offshore California. *Deep Sea Res. Part I Oceanogr. Res. Pap.* 153, 103108. doi:10.1016/j.dsr.2019.103108
- Mart, Y. (1989). Sediment Distribution in Akhziv Canyon off Northern Israel. *Geo-Mar. Lett.* 9, 77–83. doi:10.1007/bf02430427
- Martín, J., Palanques, A., and Puig, P. (2006). Composition and Variability of Downward Particulate Matter Fluxes in the Palamós Submarine Canyon (NW Mediterranean). *J. Mar. Syst.* 60, 75–97. doi:10.1016/j.jmarsys.2005.09.010
- Matos, F. L., Ross, S. W., Huvenne, V. A. I., Davies, J. S., and Cunha, M. R. (2018). Canyons Pride and Prejudice: Exploring the Submarine Canyon Research Landscape, a History of Geographic and Thematic Bias. *Prog. Oceanogr.* 169, 6–19. doi:10.1016/j.pocean.2018.04.010
- Mauffrey, M. A., Berné, S., Jouet, G., Giresse, P., and Gaudin, M. (2015). Sea-level Control on the Connection between Shelf-Edge Deltas and the Bourcart Canyon Head (Western Mediterranean) during the Last Glacial/interglacial Cycle. *Mar. Geol.* 370, 1–19. doi:10.1016/j.margeo.2015.09.010
- Mazières, A., Gillet, H., Castelle, B., Mulder, T., Guyot, C., Garlan, T., et al. (2014). High-Resolution Morphobathymetric Analysis and Evolution of Capbreton Submarine Canyon Head (Southeast Bay of Biscay—French Atlantic Coast) over the Last Decade Using Descriptive and Numerical Modelling. *Mar. Geol.* 351, 1–12. doi:10.1016/j.margeo.2014.03.001
- McArthur, A. D., and Tek, D. E. (2021). Controls on the Origin and Evolution of Deep-Ocean Trench-Axial Channels. *Geology* 49 (8), 883–888. doi:10.1130/G48612.1
- McHargue, T., Pycrc, M. J., Sullivan, M. D., Clark, J. D., Fildani, A., Romans, B. W., et al. (2011). Architecture of Turbidite Channel Systems on the Continental Slope: Patterns and Predictions. *Mar. Pet. Geol.* 28, 728–743. doi:10.1016/j.marpetgeo.2010.07.008
- Micallef, A., Mountjoy, J. J., Barnes, P. M., Canals, M., and Lastras, G. (2014). Geomorphic Response of Submarine Canyons to Tectonic Activity: Insights from the Cook Strait Canyon System, New Zealand. *Geosphere* 10 (5), 905–929. doi:10.1130/GES01040.1
- Michaud, F., Proust, J. N., Collot, J. Y., Lebrun, J. F., Witt, C., Ratzov, G., et al. (20152012). Quaternary Sedimentation and Active Faulting along the Ecuadorian Shelf: Preliminary Results of the ATACAMES Cruise. *Mar. Geophys. Res.* 36, 81–98. doi:10.1007/s11001-014-9231-y
- Milia, A. (2000). The Dohrn Canyon: A Response to the Eustatic Fall and Tectonic Uplift of the Outer Shelf along the Eastern Tyrrhenian Sea Margin. *Italy. geomar. Lett.* 20, 101–108. doi:10.1007/s003670000044
- Milliman, J. D., and Kao, S.-J. (2005). Hyperpycnal Discharge of Fluvial Sediment to the Ocean: Impact of Super-typhoon Herb (1996) on Taiwanese Rivers. *J. Geol.* 113, 503–516. doi:10.1086/431906
- Milliman, J. D., and Syvitski, P. M. (1992). Geomorphic/Tectonic Control of Sediment Discharge to the Ocean: The Importance of Small Mountainous Rivers. *J. Geol.* 100, 525–544. doi:10.1086/629606
- Mitchell, J. K., Holdgate, G. R., Wallace, M. W., and Gallagher, S. J. (2007). Marine Geology of the Quaternary Bass Canyon System, Southeast Australia: a Cool-Water Carbonate System. *Mar. Geol.* 237, 71–96. doi:10.1016/j.margeo.2006.10.037
- Molenaar, A., Moernaut, J., Wiemer, G., Dubois, N., and Strasser, M. (2019). Earthquake Impact on Active Margins: Tracing Surficial Remobilization and Seismic Strengthening in a Slope Sedimentary Sequence. *Geophys. Res. Lett.* 46, 6015–6023. doi:10.1029/2019GL082350
- Mondziel, S., Grindlay, N., Mann, P., Escalona, A., and Abrams, L. (2010). Morphology, Structure, and Tectonic Evolution of the Mona Canyon (Northern Mona Passage) from Multibeam Bathymetry, Side-Scan Sonar, and Seismic Reflection Profiles. *Tectonics* 29, TC2003. doi:10.1029/2008TC002441
- Mountjoy, J. J., Barnes, P. M., and Pettinga, J. R. (2009). Morphostructure and Evolution of Submarine Canyons across an Active Margin: Cook Strait Sector of the Hikurangi Margin, New Zealand. *Mar. Geol.* 260, 45–68. doi:10.1016/j.margeo.2009.01.006
- Mountjoy, J. J., Howarth, J. D., Orpin, A. R., Barnes, P. M., Bowden, D. A., Rowden, A. A., et al. (2018). Earthquakes Drive Large-Scale Submarine Canyon

- Development and Sediment Supply to Deep-Ocean Basins. *Sci. Adv.* 4 (3), eaar3748. doi:10.1126/sciadv.aar3748
- Mountjoy, J. J., Micallef, A., Stevens, C. L., and Stirling, M. W. (2014). Holocene Sedimentary Activity in a Non-terrestrially Coupled Submarine Canyon: Cook Strait Canyon System, New Zealand. *Deep Sea Res. Part II Top. Stud. Oceanogr.* 104, 120–133. doi:10.1016/j.dsr2.2013.09.001
- Mulder, T., Ducassou, E., Gillet, H., Hanquiez, V., Tournadour, E., Combes, J., et al. (2012). Canyon Morphology on a Modern Carbonate Slope of the Bahamas: Evidence of Regional Tectonic Tilting. *Geology* 40 (9), 771–774. doi:10.1130/G33327.1
- Mulder, T., Lecroart, P., Hanquiez, V., Marches, E., Gonthier, E., Guedes, J.-C., et al. (2006). The Western Part of the Gulf of Cadiz: Contour Currents and Turbidity Currents Interactions. *Geo-Mar. Lett.* 26 (1), 31–41. doi:10.1007/s00367-005-0013-z
- Nelson, C. H., Escutia, C., Damuth, J. E., and Twichell, D. C., Jr. (2011). “Interplay of Mass-Transport and Turbidite-System Deposits in Different Active Tectonic and Passive Continental Margin Settings: External and Local Controlling Factors,” in *Mass-Transport Deposits in Deepwater Settings*. Editors R. C. Shipp, P. Weimer, and H. W. Posamentier (Tulsa, OK: SEPM), 39–66. doi:10.2110/sepm.096.039
- NOAA National Centers for Environmental Information (2021). Available at <https://www.ncei.noaa.gov/maps/bathymetry/> [Accessed October 28, 2021]
- Noda, A., TuZino, T., Furukawa, R., Joshima, M., and Uchida, J. (2008). Physiographical and Sedimentological Characteristics of Submarine Canyons Developed upon an Active Forearc Slope: the Kushiro Submarine Canyon, Northern Japan. *Geol. Soc. Am. Bull.* 120 (5/6), 750–767. doi:10.1130/B26155.1
- Noda, A., and TuZino, T. (2010). Shelf-Slope Sedimentation during the Late Quaternary on the Southwestern Kuril Forearc Margin, Northern Japan. *Sediment. Geol.* 232, 35–51. doi:10.1016/j.sedgeo.2010.09.008
- Normark, W. R., and Carlson, P. R. (2003). “Giant Submarine Canyons: Is Size Any Clue to Their Importance in the Rock Record?,” in *Extreme depositional Environ. Mega end members Geol. time* Editors M. A. Chan and A. W. Archer (Boulder, CO: GSA), 175–190. doi:10.1130/0-8137-2370-1.175
- Normark, W. R., Piper, D. J. W., Romans, B. W., Covault, J. A., Dartnell, P., and Sliter, R. W. (2009). “Submarine Canyon and Fan Systems of the California Continental Borderland,” in *Earth Science in the Urban Ocean: The Southern California Continental Borderland*. Editors H. J. Lee and W. R. Normark (Boulder, CO: GSA), 141–168. doi:10.1130/2009.2454(2.7)
- Normark, W. R., Posamentier, H., and Mutti, E. (1993). Turbidite Systems: State of the Art and Future Directions. *Rev. Geophys.* 31 (2), 91–116. doi:10.1029/93rg02832
- Nyberg, B., Helland-Hansen, W., Gawthorpe, R. L., Sandbakken, P., Eide, C. H., Somme, T., et al. (2018). Revisiting Morphological Relationships of Modern Source-To-Sink Segments as a First-Order Approach to Scale Ancient Sedimentary Systems. *Sediment. Geol.* 373, 111–133. doi:10.1016/j.sedgeo.2018.06.007
- Oiwane, H., Tonai, S., Kiyokawa, S., Nakamura, Y., Suganuma, Y., and Tokuyama, H. (2011). Geomorphological Development of the Goto Submarine Canyon, Northeastern East China Sea. *Mar. Geol.* 288, 49–60. doi:10.1016/j.margeo.2011.06.013
- Palanques, A., El Khatab, M., Puig, P., Masqué, P., Sánchez-Cabeza, J. A., and Isla, E. (2005). Downward Particle Fluxes in the Guadiaro Submarine Canyon Depositional System (North-western Alboran Sea), a River Flood Dominated System. *Mar. Geol.* 220, 23–40. doi:10.1016/j.margeo.2005.07.004
- Palanques, A., Martín, J., Puig, P., Guillén, J., Company, J. B., and Sardá, F. (2006). Evidence of Sediment Gravity Flows Induced by Trawling in the Palamós (Fonera) Submarine Canyon (Northwestern Mediterranean). *Deep Sea Res. Part I Oceanogr. Res. Pap.* 53, 201–214. doi:10.1016/j.dsr.2005.10.003
- Paull, C. K., Caress, D. W., Lundsten, E., Gwiazda, R., Anderson, K., McGann, M., et al. (2013). Anatomy of the La Jolla Submarine Canyon System; Offshore Southern California. *Mar. Geol.* 335, 16–34. doi:10.1016/j.margeo.2012.10.003
- Peakall, J., and Sumner, E. J. (2015). Submarine Channel Flow Processes and Deposits: a Process-Product Perspective. *Geomorphology* 244, 95–120. doi:10.1016/j.geomorph.2015.03.005
- Pierau, R., Hanebuth, T. J. J., Krastel, S., and Henrich, R. (2010). Late Quaternary Climatic Events and Sea-Level Changes Recorded by Turbidite Activity, Dakar Canyon, NW Africa. *Quat. Res.* 73, 385–392. doi:10.1016/j.yqres.2009.07.010
- Pierau, R., Henrich, R., Preiß-Daimler, I., Krastel, S., and Geersen, J. (2011). Sediment Transport and Turbidite Architecture in the Submarine Dakar Canyon off Senegal, NW-Africa. *J. Afr. Earth Sci.* 60, 196–208. doi:10.1016/j.jafrearsci.2011.02.010
- Pierdomenico, M., Casalbore, D., and Chiocci, F. L. (2019). Massive Benthic Litter Funnelled to Deep Sea by Flash-Flood Generated Hyperpycnal Flows. *Sci. Rep.* 9, 5530. doi:10.1038/s41598-019-41816-8
- Pierdomenico, M., Martorelli, E., Dominguez-Carrío, C., Gili, J. M., and Chiocci, F. L. (2016). Seafloor Characterization and Benthic Megafaunal Distribution of an Active Submarine Canyon and Surrounding Sectors: The Case of Gioia Canyon (Southern Tyrrhenian Sea). *J. Mar. Syst.* 157, 101–117. doi:10.1016/j.jmarsys.2016.01.005
- Piper, D. J. W., Hiscott, R. N., and Normark, W. R. (1999). Outcrop-scale Acoustic Facies Analysis and Latest Quaternary Development of Hueneme and Dume Submarine Fans, Offshore California. *Sedimentology* 46, 47–78. doi:10.1046/j.1365-3091.1999.00203.x
- Piper, D. J. W., and Normark, W. R. (2009). Processes that Initiate Turbidity Currents and Their Influence on Turbidites: a Marine Geology Perspective. *J. Sediment. Res.* 79, 347–362. doi:10.2110/jsr.2009.046
- Pisareva, M. N., Pickart, R. S., Lin, P., Fratantoni, P. S., and Weingartner, T. J. (2019). On the Nature of Wind-Forced Upwelling in Barrow Canyon. *Deep Sea Res. Part II Top. Stud. Oceanogr.* 162, 63–78. doi:10.1016/j.dsr2.2019.02.002
- Popescu, I., Lericolais, G., Panin, N., Normand, A., Dinu, C., and Le Drezen, E. (2004). The Danube Submarine Canyon (Black Sea): Morphology and Sedimentary Processes. *Mar. Geol.* 206, 249–265. doi:10.1016/j.margeo.2004.03.003
- Pratson, L. F., Nittrouer, C. A., Wiberg, P. L., Steckler, M. S., Swenson, J. B., Cacchione, D. A., et al. (2007). “Seascape Evolution on Clastic Continental Shelves and Slopes,” in *Continental Margin Sedimentation: From Sediment Transport to Sequence Stratigraphy*. Editors C. A. Nittrouer, J. A. Austin, M. E. Field, J. H. Kravitz, J. P. M. Syvitski, and P. L. Wiberg (Oxford, UK: Blackwell Publishing), 339–380.
- Puga-Bernabéu, A., Webster, J. M., Beaman, R. J., and Guilbaud, V. (2011). Morphology and Controls on the Evolution of a Mixed Carbonate-Siliciclastic Submarine Canyon System, Great Barrier Reef Margin, North-Eastern Australia. *Mar. Geol.* 289, 100–116. doi:10.1016/j.margeo.2011.09.013
- Puig, P., Durán, R., Muñoz, A., Elvira, E., and Guillén, J. (2017). Submarine Canyon-Head Morphologies and Inferred Sediment Transport Processes in the Alías-Almanzora Canyon System (SW Mediterranean): on the Role of the Sediment Supply. *Mar. Geol.* 393, 21–34. doi:10.1016/j.margeo.2017.02.009
- Puig, P., Palanques, A., Guillén, J., and García-Ladona, E. (2000). Deep Slope Currents and Suspended Particle Fluxes in and Around the Foix Submarine Canyon (NW Mediterranean). *47. Deep Sea Res. Part I Oceanogr. Res. Pap.* 47, 343343–366366. doi:10.1016/s0967-0637(99)00062-x
- Puig, P., Palanques, A., and Martín, J. (2014). Contemporary Sediment-Transport Processes in Submarine Canyons. *Annu. Rev. Mar. Sci.* 6, 53–77. doi:10.1146/annurev-marine-010213-135037
- Ratzov, G., Sosson, M., Collot, J.-Y., and Migeon, S. (2012). Late Quaternary Geomorphologic Evolution of Submarine Canyons as a Marker of Active Deformation on Convergent Margins: The Example of the South Colombian Margin. *Mar. Geol.* 315–318, 77–97. doi:10.1016/j.margeo.2012.05.005
- Reid, I., and Frostick, L. E. (2011). “Chapter 13: Channel Form, Flows and Sediments of Endogenous Ephemeral Rivers in Deserts,” in *Arid Zone Geomorphology: Process, Form and Change in Drylands*. Editor D. S. G. Thomas (Oxford, UK: John Wiley & Sons), 301–332. doi:10.1002/978047010777.ch13
- Restrepo-Correa, I. C., and Ojeda, G. Y. (2010). Geologic Controls on the Morphology of La Aguja Submarine Canyon. *J. South. Am. Earth. Sci.* 29, 861–870. doi:10.1016/j.jsames.2010.07.001
- Ridente, D., Martorelli, E., Bosman, A., and Chiocci, F. L. (2014). High-resolution Morpho-Bathymetric Imaging of the Messina Strait (Southern Italy). New Insights on the 1908 Earthquake and Tsunami. *Geomorphology* 208, 149–159. doi:10.1016/j.geomorph.2013.11.021
- Rise, L., Boe, R., Riis, F., Bellec, V. K., Laberg, J. S., Eidvin, T., et al. (2013). The Lofoten-Vesterålen Continental Margin, North Norway: Canyons and Mass-

- Movement Activity. *Mar. Pet. Geol.* 45, 134–149. doi:10.1016/j.marpetgeo.2013.04.021
- Rona, P., Guida, V., Scranton, M., Gong, D., Macelloni, L., Pierdomenico, M., et al. (2015). Hudson Submarine Canyon Head Offshore New York and New Jersey: A Physical and Geochemical Investigation. *Deep Sea Res. Part II Top. Stud. Oceanogr.* 121, 213–232. doi:10.1016/j.dsr2.2015.07.019
- Rowan, M. G., Peel, F. J., and Vendeville, B. C. (2004). “Gravity-driven Fold Belts on Passive Margins,” in *Thrust Tectonics and Hydrocarbon Systems*. Editor K. R. McClay (Tulsa, OK: AAPG), 157–182.
- Salmanidou, D. M., Heidarzadeh, M., and Guillas, S. (2019). Probabilistic Landslide-Generated Tsunamis in the Indus Canyon, NW Indian Ocean, Using Statistical Emulation. *Pure Appl. Geophys.* 176, 3099–3114. doi:10.1007/s00024-019-02187-3
- Sanchez, C. M., Fulthorpe, C. S., and Steel, R. J. (2012). Miocene Shelf-Edge Deltas and Their Impact on Deepwater Slope Progradation and Morphology, Northwest Shelf of Australia. *Basin Res.* 24, 683–698. doi:10.1111/j.1365-2117.2012.00545.x
- Santora, J. A., Zeno, R., Dorman, J. G., and Sydeman, W. J. (2018). Submarine Canyons Represent an Essential Habitat Network for Krill Hotspots in a Large Marine Ecosystem. *Sci. Rep.* 8, 7579. doi:10.1038/s41598-018-25742-9
- Sawyer, D. E., and DeVore, J. R. (2015). Elevated Shear Strength of Sediments on Active Margins: Evidence for Seismic Strengthening. *Geophys. Res. Lett.* 42, 10216–10221. doi:10.1002/2015GL066603
- Schnürle, P., Liu, C.-S., Lallemand, S. E., and Reed, D. (1998). Structural Controls of the Taitung Canyon in the Huatung Basin East of Taiwan. *TAO* 9 (3), 453–472.
- Shumaker, L. E., Jobe, Z. R., Johnstone, S. A., Pettinga, L. A., Cai, D. X., and Moody, J. D. (2018). Controls on Submarine Channel-Modifying Processes Identified through Morphometric Scaling Relationships. *Geosphere* 14 (5), 2171–2187. doi:10.1130/GES01674.1
- Shyu, J. B. H., Sieh, K., and Chen, Y.-G. (2005). Tandem Suturing and Disarticulation of the Taiwan Orogen Revealed by its Neotectonics Elements. *Earth Planet. Sci. Lett.* 233, 167–177. doi:10.1016/j.epsl.2005.01.018
- Smith, M. E., Finnegan, N. J., Mueller, E. R., and Best, R. J. (2017). Durable Terrestrial Bedrock Predicts Submarine Canyon Formation. *Geophys. Res. Lett.* 44, 10332–10340. doi:10.1002/2017GL075139
- Soh, W., Tokuyama, H., Fujioka, K., Kato, S., and Taira, A. (1990). Morphology and Development of a Deep-Sea Meandering Canyon (Boso Canyon) on an Active Plate Margin, Sagami Trough, Japan. *Mar. Geol.* 91, 227–241. doi:10.1016/0025-3227(90)90038-1
- Soh, W., and Tokuyama, H. (2002). Rejuvenation of Submarine Canyon Associated with Ridge Subduction, Tenryu Canyon, off Tokai, Central Japan. *Mar. Geol.* 187, 203–220. doi:10.1016/s0025-3227(02)00267-0
- Sømme, T. O., Helland-Hansen, W., Martinsen, O. J., and Thurmond, J. B. (2009). Relationships between Morphological and Sedimentological Parameters in Source-to-Sink Systems: A Basis for Predicting Semi-quantitative Characteristics in Subsurface Systems. *Basin Res.* 21, 361–387. doi:10.1111/j.1365-2117.2009.00397.x
- Soulet, W., Migeon, S., Gorini, C., Rubino, J.-L., Raison, F., and Bourges, P. (2016). Erosional versus Aggradational Canyons along a Tectonically-Active Margin: the Northeastern Ligurian Margin (Western Mediterranean Sea). *Mar. Geol.* 382, 17–36. doi:10.1016/j.margeo.2016.09.015
- Soutter, E. L., Bell, D., Cumberpatch, Z. A., Ferguson, R. A., Sychala, Y. T., Kane, I. A., et al. (2020). The Influence of Confining Topography Orientation on Experimental Turbidity Currents and Geological Implications. *Earth Sci.* 8, 540633.
- Soutter, E. L., Kane, I. A., Hodgson, D. M., and Flint, S. (2021). The Concavity of Submarine Canyon Longitudinal Profiles. *J. Geophys. Res. Earth. Surf.* 126, e2021JF006185. doi:10.1029/2021JF006185
- Stow, D. (1986). “Deep Clastic Seas,” in *Sedimentary Environments and Facies*. Editor H. G. Reading (Boston, MA: Blackwell), 399–443.
- Strozyk, F., Strasser, M., Förster, A., Kopf, A., and Huhn, K. (2010). Slope Failure Repetition in Active Margin Environments: Constraints from Submarine Landslides in the Hellenic Fore Arc, Eastern Mediterranean. *J. Geophys. Res. Earth.* 115, B08103. doi:10.1029/2009JB006841
- Su, M., Hsiung, K.-H., Zhang, C., Xie, X., Yu, H.-S., and Wang, Z. (2015). The Linkage between Longitudinal Sediment Routing Systems and Basin Types in the Northern South China Sea in Perspective of Source-To-Sink. *J. Asian Earth Sci.* 111, 1–13. doi:10.1016/j.jseas.2015.05.011
- Su, M., Lin, Z., Wang, C., Kuang, Z., Liang, J., Chen, H., et al. (2020). Geomorphologic and Infilling Characteristics of the Slope-Confining Submarine Canyons in the Pearl River Mouth Basin, Northern South China Sea. *Mar. Geol.* 424, 106166. doi:10.1016/j.margeo.2020.106166
- Susanth, S., Kurian, P. J., Bijesh, C. M., Twinkle, D., Tyagi, A., and Rajan, S. (2021). Controls on the Evolution of Submarine Canyons in Steep Continental Slopes: Geomorphological Insights from Palar Basin, Southeastern Margin of India. *Geo-Mar. Lett.* 41, 14. doi:10.1007/s00367-021-00685-9
- Sweet, M. L., and Blum, M. D. (2016). Connections between Fluvial to Shallow Marine Environments and Submarine Canyons: Implications for Sediment Transfer to Deep Water. *J. Sediment. Res.* 86, 1147–1162. doi:10.2110/jsr.2016.64
- Sylvester, Z., Deptuck, M., Prather, B. E., Pirmez, C., and O’Byrne, C. (2012). “Seismic Stratigraphy of a Shelf-Edge Delta and Linked Submarine Channels in the Northeastern Gulf of Mexico,” in *Application of the Principles of Seismic Geomorphology to Continental Slope and Base-Of-Slope Systems: Case Studies from Seafloor and Near-Seafloor Analogues*. Editors B. E. Prather, M. E. Deptuck, D. Mohrig, B. Van Hooen, and R. B. Wynn (Tulsa, OK: SEPM), 31–59. doi:10.2110/pec.12.99.0031
- Thornburg, T. M., Kulm, L. D., and Hussong, D. M. (1990). Submarine-fan Development in the Southern Chile Trench: A Dynamic Interplay of Tectonics and Sedimentation. *Am. Geol. Soc. Bull.* 102, 1658–1680. doi:10.1130/0016-7606(1990)102<1658:sfdits>2.3.co;2
- Trumbull, J. V. A., and Garrison, L. E. (1973). Geology of a System of Submarine Canyons South of Puerto Rico. *J. Res. U.S. Geol. Surv.* 1 (3), 293–299.
- Tubau, X., Lastras, G., Canals, M., Micallef, A., and Amblas, D. (2013). Significance of the Fine Drainage Pattern for Submarine Canyon Evolution: the Foix Canyon System, Northwestern Mediterranean Sea. *Geomorphology* 184, 20–37. doi:10.1016/j.geomorph.2012.11.007
- Tubau, X., Paull, C. K., Lastras, G., Caress, D. W., Canals, M., Lundsten, E., et al. (2015). Submarine Canyons of Santa Monica Bay, Southern California: Variability in Morphology and Sedimentary Processes. *Mar. Geol.* 365, 61–79. doi:10.1016/j.margeo.2015.04.004
- TuZino, T., and Noda, A. (2010). Architecture and Evolution of the Kuroshio Submarine Canyon in the Kurile Trench Forearc Slope, North-western Pacific. *Sedimentology* 57, 611–641. doi:10.1111/j.1365-3091.2009.01107.x
- Urias Espinosa, J., Bandy, W. L., Mortera Gutiérrez, C. A., Núñez Cornú, F. J., and Mitchell, N. C. (2016). Multibeam Bathymetric Survey of the Ipala Submarine Canyon, Jalisco, Mexico (20°N): The Southern Boundary of the Banderas Forearc Block? *Tectonophysics* 671, 249–263. doi:10.1016/j.tecto.2015.12.029
- Valentine, P. C., Uzzmann, J. R., and Cooper, R. A. (1980). Geology and Biology of Oceanographer Submarine Canyon. *Mar. Geol.* 38, 283–312. doi:10.1016/0025-3227(80)90004-3
- Vardar, D. (2019). Morphological Definition of the North İmralı Canyon in the Sea of Marmara. *Arab. J. Geosci.* 12, 76. doi:10.1007/s12517-019-4257-8
- von Rad, U., and Tahir, M. (1997). Late Quaternary Sedimentation on the Outer Indus Shelf and Slope (Pakistan): Evidence from High-Resolution Seismic Data and Coring. *Mar. Geol.* 138, 193–236. doi:10.1016/s0025-3227(96)00090-4
- Walsh, J. P., Alexander, C. R., Gerber, T., Orpin, A. R., and Sumners, B. W. (2007/2007). Demise of a Submarine Canyon? Evidence for Highstand Infilling on the Waipaoa River Continental Margin, New Zealand. *Geophys. Res. Lett.* 34, L20606. doi:10.1029/2007GL031142
- Wan, L., Bianchi, V., Hurter, S., Salles, T., Zhang, Z., and Yuan, X. (2021). Morphological Controls on Delta-Canyon-Fan Systems: Insights from Stratigraphic Forward Models. *Sedimentol. Early View* 2021. doi:10.1111/sed.12930
- Wang, R., Colomera, L., and Mountney, N. P. (2019). Geological Controls on the Geometry of Incised-Valley Fills: Insights from a Global Dataset of Late-Quaternary Examples. *Sedimentology* 66 (6), 2134–2168. doi:10.1111/sed.12596
- Warratz, G., Schwenk, T., Voigt, I., Bozzano, G., Henrich, R., Violante, R., et al. (2019). Interaction of a deep-sea current with a blind submarine canyon (Mar del Plata Canyon, Argentina). *Mar. Geol.* 417, 106002. doi:10.1016/j.margeo.2019.106002
- Wiles, E., Green, A., Watkeys, M., Jokat, W., and Krockner, R. (2013). The Evolution of the Tugela Canyon and Submarine Fan: a Complex Interaction between Margin Erosion and Bottom Current Sweeping, Southwest Indian Ocean, South Africa. *Mar. Pet. Geol.* 44, 60–70. doi:10.1016/j.marpetgeo.2013.03.012
- Wynn, R. B., Weaver, P. P. E., Masson, D. G., and Stow, D. A. V. (2002). Turbidite Depositional Architecture across Three Interconnected Deep-Water Basins on

- the North-West African Margin. *Sedimentology* 49, 669–695. doi:10.1046/j.1365-3091.2002.00471.x
- Xu, J. P., and Noble, M. A. (2009). Currents in Monterey Submarine Canyon. *J. Geophys. Res.* 114, C03004. doi:10.1029/2008JC004992
- Xu, S., Wang, Y., Peng, X., Zou, H., Qiu, Y., Gong, C., et al. (2014). Origin of Taiwan Canyon and its Effects on Deepwater Sediment. *Sci. China Earth Sci.* 57 (11), 2769–2780. doi:10.1007/s11430-014-4942-0
- Yang, X., Peel, F. J., McNeill, L. C., and Sanderson, D. J. (2020). Comparison of Fold-Thrust Belts Driven by Plate Convergence and Gravitational Failure. *Earth-Sci. Rev.* 203, 103136. doi:10.1016/j.earscirev.2020.103136
- Yin, S., Li, J., Ding, W., Gao, J., Ding, W., and Wang, Y. (2018). Migration of the Lower North Palawan Submarine Canyon: Characteristics and Controls. *Int. Geol. Rev.* 6287-8, 988–1005. doi:10.1080/00206814.2018.1522519
- Yin, S., Wang, L., Guo, Y., and Zhong, G. (2015). Morphology, Sedimentary Characteristics, and Origin of the Dongsha Submarine Canyon in the Northeastern Continental Slope of the South China Sea. *Sci. China Earth Sci.* 58, 971–985. doi:10.1007/s11430-014-5044-8
- Yu, H.-S., and Chang, J.-F. (2002). The Penghu Submarine Canyon off Southwestern Taiwan: Morphology and Origin. *Terr. Atmos. Ocean. Sci.* 13 (4), 547–562. doi:10.3319/tao.2002.13.4.547(o)
- Yu, H.-S., and Chiang, C.-S. (1995). Morphology and Origin of the Hongtsai Submarine Canyon West of the Hengchun Peninsula, Taiwan. *J. Geol. Soc. China.* 38 (1), 81–93.
- Yu, H.-S., Liu, C. S., and Lee, J.-T. (1992). The Kaohsiung Submarine Canyon: a Modern Aborted Canyon and its Morphology and Echo Character. *Acta Ocean. Taiwan* 28, 19–30.
- Yu, H.-S., and Lu, J. C. (1995). Development of the Shale Diapir-Controlled Fangliao Canyon on the Continental Slope off Southwestern Taiwan. *J. Asian Earth Sci.* 11 (4), 265–276. doi:10.1016/0743-9547(95)00004-c
- Zavala, C. (2020). Hyperpycnal (Over Density) Flows and Deposits. *J. Palaeogeogr.* 9, 17. doi:10.1186/s42501-020-00065-x
- Zhang, F., Hu, Y., Fan, X., Yu, W., Liu, X., and Jin, Z. (2022). Controls on Seasonal Erosion Behavior and Potential Increase in Sediment Evacuation in the Warming Tibetan Plateau. *Catena* 209, 105797. doi:10.1016/j.catena.2021.105797
- Zhang, Y., Liu, Z., Zhao, Y., Colin, C., Zhang, X., Wang, M., et al. (2018). Long-term *In Situ* Observations on Typhoon-Triggered Turbidity Currents in the Deep Sea. *Geology* 46 (8), 675–678. doi:10.1130/G45178.1
- Zhong, G., and Peng, X. (2021). Transport and Accumulation of Plastic Litter in Submarine Canyons – The Role of Gravity Flows. *Geology* 49, 581–586. doi:10.1130/G48536.1

Conflict of Interest: The authors declare that the research was conducted in the absence of any commercial or financial relationships that could be construed as a potential conflict of interest.

Publisher's Note: All claims expressed in this article are solely those of the authors and do not necessarily represent those of their affiliated organizations, or those of the publisher, the editors and the reviewers. Any product that may be evaluated in this article, or claim that may be made by its manufacturer, is not guaranteed or endorsed by the publisher.

Copyright © 2022 Bührig, Colombera, Patacci, Mountney and McCaffrey. This is an open-access article distributed under the terms of the Creative Commons Attribution License (CC BY). The use, distribution or reproduction in other forums is permitted, provided the original author(s) and the copyright owner(s) are credited and that the original publication in this journal is cited, in accordance with accepted academic practice. No use, distribution or reproduction is permitted which does not comply with these terms.